Forced-self-excited System of Iced Transmission Lines under Planar Harmonic Excitations

Xiaohui Liu
State Key Laboratory of Mountain Bridge and Tunnel Engineering, Chongqing Jiaotong University
Shuguang Yang (622180970178@mails.cqjtu.edu.cn)
Chongqing Jiaotong University, School of Civil Engineering https://orcid.org/0000-0002-4554-4795
Guangyun Min
Chongqing Jiaotong University, School of Civil Engineering
Ceshi Sun
State Key Laboratory of Mountain Bridge and Tunnel Engineering, Chongqing Jiaotong University
Haobo Liang
Chongqing Jiaotong University, School of Civil Engineering
Ming Zou
Chongqing Jiaotong University, School of Civil Engineering
Chuan Wu
State Grid Henan Electric Power Research Institute
Mengqi Cai
Chengdu University, School of Architecture and Civil Engineering

Research Article

Keywords: Principal resonance, Harmonic resonance, Approximate analytical solution, Quenching phenomenon, Iced transmission lines, Forced-self-excited system

Posted Date: April 26th, 2021

DOI: https://doi.org/10.21203/rs.3.rs-430539/v1

Forced-self-excited System of Iced Transmission Lines under Planar Harmonic Excitations

Xiaohui Liu [1], Shuguang Yang [2*], Guangyun Min [2], Ceshi Sun [1], Haobo Liang [2], Ming Zou [2], Chuan Wu [3], Mengqi Cai [4]

1. Associate Professor, State Key Laboratory of Mountain Bridge and Tunnel Engineering, Chongqing Jiaotong University, Chongqing 400074, People's Republic of China. (E-mail: cqdxlxh@126.com; suncs1984@163.com)
2. Graduate Student, School of Civil Engineering, Chongqing Jiaotong University, Chongqing 400074, People's Republic of China. (E-mail: Corresponding Author, 622180970178@mails.cqjtu.edu.cn; guangyunmin@163.com; Haoboliang0816@163.com; 622180970089@mails.cqjtu.edu.cn)
3. Senior Engineer, State Grid Henan Electric Power Research Institute, Zhengzhou 450052, People's Republic of China. (E-mail: wuchuan77415@aliyun.com)
4. Associate Professor, School of Architecture and Civil Engineering, Chengdu University, Chengdu 610106, People's Republic of China. (E-mail: mq.cai@foxmail.com)

Abstract: This paper is concerned with the analysis of the self-excited vibrations and forced vibrations of the iced transmission lines. By introducing the external excitation load, the effect of dynamic wind on the nonlinear vibration equations of motion is reflected by vertical aerodynamic force. The approximate analytical solution of the non-resonance, and the amplitude frequency response relation of the principal resonance of the forced self-excited system are obtained by using the multiple scale method. With the increase in excitation amplitude, the nonlinearity of the system is enhanced, and the forced-self-excited system experiences three vibration stages (self-excited vibration, the superposition form of self-excited vibration and forced vibration, forced vibration controlled by nonlinear damping). Among them, the accuracy of the approximate analytical solution decreases with the increase of the nonlinear strength. And the excitation amplitude is greater than the critical value, the quenching phenomenon appear in the forced-self-excited system, and the discriminant formula is derived in this paper. In addition, the frequency of excitation term determines the vibration form of the system. The principal resonance, super-harmonic resonance and sub-harmonic resonance of the forced-self-excited system are analyzed by using different excitation frequencies. Compared with the principal resonance and the harmonic resonance, the meaningful transition from periodic response to quasi periodic response is easy to appear with the condition of the 1/3-order sub-harmonic and the 3-order super-harmonic. The conclusions would be helpful to the practical engineering of the iced transmission lines. More important, as a combination of Duffing

equation and Rayleigh equation, the forced-self-excited system also has high theoretical research value.

Key words: Principal resonance; Harmonic resonance; Approximate analytical solution; Quenching phenomenon; Iced transmission lines; Forced-self-excited system

1 Introduction

Galloping of iced transmission line is a typical self-excited vibration [1]. Under the excitation of wind load, the iced transmission line is prone to galloping of long time [2]. Therefore, the iced transmission line structure may make short circuit, frequent tripping, broken strand or wire and other accidents [3]. Thus, to some extent, the research on the nonlinear characteristics of transmission line galloping has very important engineering application value and theoretical research significance.

The iced transmission line belongs to suspended elastic cables，and the stay cable of cable-stayed bridge also belongs to cable structure. Therefore, both transmission lines and stay-cables belong to cable structure. Under the action of external excitation, the phenomenon of rain-wind induced galloping [4], dry-galloping [5] and ice-galloping will appear in the stay cable of cable-stayed bridge.

In recent years, cable structure has been studied by many scholars. Firstly, some scholars have studied suspended elastic cables and stay cables. Arafat and Nayfeh [6] investigated the non-linear forced responses of shallow suspended cables, which mainly include the case of principal resonance and auto-parametric resonance. According to the different excitation forms of cable structures, the dynamics response (internal resonance response, principal resonances response, harmonic resonance response) of system may be excited [7-9]. For example, under the condition of external excitation, Nayfeh et al. [10] studied the nonlinear nonplanar response of the suspended cable by considering different symmetrical modes and different internal resonance conditions. Under the condition of harmonic excitation, Rega and Benedettini [11, 12] studied the plane nonlinear dynamics response (sub-harmonic resonance and super-harmonic resonance) of elastic cable. Under the condition of parametric excitation and external excitation, Chen et al. [13] and Zhang et al. [14] studied the bifurcation and chaotic dynamics of suspension cable. In addition, the cable structure with different boundary motion conditions will also generate different nonlinear dynamic characteristics. For example, Perkins et al. [15] established a theoretical model of suspension cable excited by support vibration. And combined with experiments and theoretical analysis, it is proved that internal resonance will reduce the plane stability of the system. Sun et al. [16] studied the influence of different phase support excitation on the response of suspension cable. Berlioz and Lamarque [17] carried out theoretical and experimental research on stay cables, and proposed a model to predict nonlinear

behavior. Based on the modified Irvine formula, Wu et al. [18] derived the formula of the inclined cable with small sag, which can be used to calculate in-plane natural frequencies and the modes shapes. The reference [6-18] mainly studies the nonlinear vibration response characteristics of cable structure, such as principal resonance, internal resonance and harmonic resonance by the experimental verification and theoretical modeling analysis. However, the nonlinear behavior of cable structure to dynamic wind is rarely studied. Additional, Daniele and Luongo [19, 20] considered the dynamics of two towers exposed to turbulent wind flow and linked by a nonlinear viscous device. And stated the steady component of the wind is responsible for self-excitation, while the turbulent part causes both parametric and external excitations, considered in a specific resonance condition.

Combined with the analysis of reference [6-20], the nonlinear galloping characteristics of iced transmission lines under dynamic wind are studied in this paper. And the hysteretic nonlinear restoring force term are considered, which include the quadratic and cubic nonlinear terms, and the Rayleigh damping term. For the reference [21], the influence of dynamic wind on the structure of iced transmission line had been studied by analyzed forced-self-excited system, and the nonlinear response characteristics under different harmonic excitation are discussed. Based on the research of reference [21], this paper discusses the influence of different excitation amplitudes on the forced-self-excited system, and make a systematic analysis on the harmonic resonance of the forced-self-excited system by the numerical solution. With the increase in excitation amplitude, the vibration form of forced-self-excited system has three stages: (1) pure self-excited vibration (excitation amplitude is equal to 0); (2) superposition form of self-excited vibration and forced vibration; (3) forced vibration affected by Rayleigh damping-- quenching phenomenon (the excitation amplitude is greater than the critical value). At the same time, it is found that the damage level of different resonance forms to the iced transmission line system by the numerical analysis: principal resonance > super-harmonic resonance > sub-harmonic resonance. The conclusion obtained by this paper would be helpful to the nonlinear galloping analysis of iced transmission lines, and could also give some references to practical engineering.

This paper is organized as follows: in section 2, under the condition of dynamic wind, the mathematical formulation of iced transmission line system (forced-self-excited system) is given. And the nonlinear galloping governing equation of the system is obtained by using Galerkin method. In section 3, the approximate analytical solution of the forced-self-excited system is obtained by using the multiple scale method, and the three vibration stages of the system are analyzed. In section 4, the amplitude frequency response relation of weak nonlinear system is obtained by multiple scale method, and the accuracy of analytical solution is verified by numerical solution. In section 5, the Runge Kutta function is used to obtain the nonlinear response of the forced-self-excited system under harmonic

excitation with different frequency, and the system dynamics response under different excitation amplitude is analyzed systematically. A detailed summary of the results is presented in section 6.

2 Dynamic Model of Iced Transmission Lines

This paper uses the same physical model as reference [21]. Fig. 1 is the model of singe-span equal-height transmission lines, and in Fig. 1, $u(s,t)$, $v(s,t)$ are the displacements measured form the dynamic equilibrium configuration in the x-axis and y-axis directions respectively and $p^*\cos(\Omega t)$ is the forced excitation load. Considering the iced transmission lines have a small initial sag-to-span ratio (less than 1:8) and low static strain, the associated static equilibrium configuration of the iced transmission lines can be described through the parabola $y=4d[s/L-(s/L)^2]$ (s is the curvilinear abscissa; L is the span length; d is the sag) [22]. In addition, the initial static equilibrium configuration is ξ_1, and the dynamic equilibrium configuration is ξ_2. And it is considered that the wind is along the z-axis direction as shown in Fig. 2.

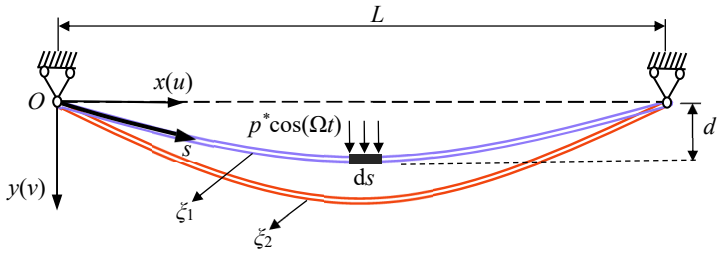

Fig. 1 The model of singe-span equal-height transmission lines

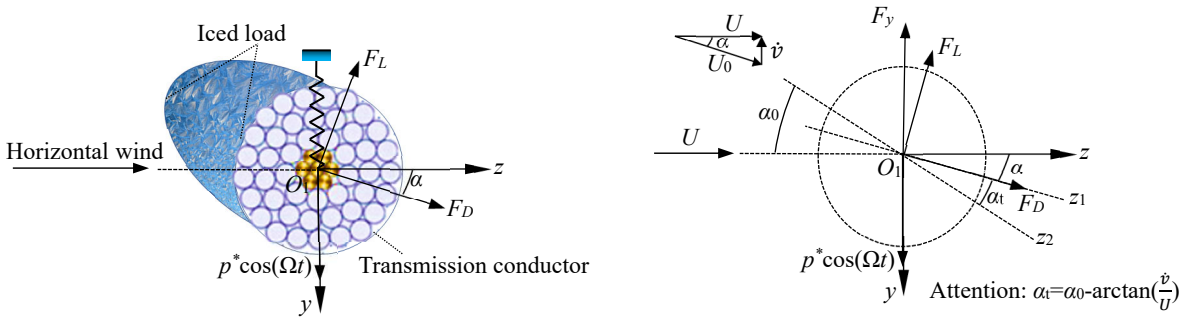

(a) The physical model (b) The force analysis model

Fig. 2 The model of cross-section of iced transmission lines

Based on quasi-static assumption, Fig. 2 is the model of cross-section of iced transmission lines, and Fig. 2(a) is the physical model of the iced transmission line cross section, and Fig. 2(b) is the force analysis model of the iced transmission line cross section; the O_1z_2 is the symmetry axis of cross-section of iced transmission lines, O_1z_1 is the direction in which the horizontal wind acts on the

iced transmission line during vibration, O_1z is the horizontal axis, α is wind attack angle, α_0 is initial wind attack angle, α_t is relative wind attack angle, U is horizontal wind velocity, U_0 is relatively wind velocity and $\dot{v}$ is the vertical vibration velocity.

From Fig. 2, it can be obtained that

$$\tan(\alpha) = \dot{v} / U \approx \alpha \tag{1}$$

The relative wind acts on the iced transmission lines, which results in an air drag (F_D) along the relative wind direction and an upward air lift (F_L) perpendicular to the relative wind direction. According to fluid-induced vibration theory, the expressions of F_L and F_D can be listed [23]:

$$F_L = \rho U^2 D C_L / 2 \tag{2a}$$

$$F_D = \rho U^2 D C_D / 2 \tag{2b}$$

where C_L is the lift coefficient of aerodynamic, C_D is the drag coefficient of aerodynamic, ρ is the air density and D is the diameter of the iced transmission line.

According to equation (1-2), it can be obtained that [21]:

$$F_y = F_L \cos(\alpha) - F_D \sin(\alpha) = \rho U^2 D C_y / 2 \tag{3}$$

Considering small deformation, that is, $\sin(\alpha) \approx \alpha$, $\cos(\alpha) \approx 1$. Based on the Taylor' law, the aerodynamic coefficients (C_y) in the y axis direction can be fitted with a cubic nonlinear curve:

$$C_y = C_0 + A'\alpha + B'\alpha^3 + C'\alpha^2 \tag{4}$$

where C_y, A', B' and C' is undetermined coefficients related to the aerodynamic loads. The coefficient C_0 has nothing to do with the vertical vibration velocity $\dot{v}$, and the coefficient C' has nothing to do with the wind velocity, so only the aerodynamic fitting coefficients A' and B' are considered.

Under the continuous excitation of the wind excitation, the iced transmission line will have self-excited vibration with constant amplitude. However, in practice, dynamic wind is unstable. Based on this concept, combined equation (1-4) and reference [21], the vertical aerodynamic force of dynamic wind is:

$$F_{y1} = \tilde{a}\dot{v} + \tilde{b}\dot{v}^3 - p^* \bullet \cos(\Omega t) \tag{5}$$

According to the nonlinear vibration theory, when the response contains sub-harmonic and super-harmonic components, the relationship between the restoring force term and the displacement of the system is a non-linear closed curve, which has obvious nonlinear hysteresis characteristics. The simplified vertical aerodynamic force $F_{y1} = \tilde{a}\dot{v} + \tilde{b}\dot{v}^3 - p^* \bullet \cos(\Omega t)$ of dynamic wind includes the external excitation term $-p^* \bullet \cos(\Omega t)$ and the Rayleigh damping term $\tilde{a}\dot{v} + \tilde{b}\dot{v}^3$. The Rayleigh damping term, quadratic, and cubic nonlinear restoring force term constitute the nonlinear hysteresis force of the system. The stable part of dynamic wind is injected into the iced transmission line to generate self-

excited vibration, and the unstable part will cause external excitation [19-20]. In equation (5), the average wind (stable part) in the natural wind is expressed as Rayleigh damping term $\tilde{a}\dot{v}+\tilde{b}\dot{v}^3$, and the unstable part in the natural wind is simplified as the external excitation term's effect on the iced transmission line system. The parameters in Equation (5) are as follows:

$$\tilde{a}=\rho UDA'/2,\quad \tilde{b}=\rho DB'/2U \tag{6}$$

According to the vertical galloping mechanism proposed by Den Hartog in reference [24, 29], and combined with equation (5), it is easy to give the governing equation of the vertical movement of the iced transmission line under the action of dynamic wind:

$$\{Hv'+ES(y'+v')\int_0^l[y'v'+v'^2/2]\mathrm{d}x\}'-F_y+p^*\bullet\cos(\Omega t)-\mu\dot{v}=m\ddot{v} \tag{7}$$

where H is the tension of the iced transmission lines, E is the Young's Modulus of the iced transmission lines, and S is the cross-sectional area of the iced transmission line. v' is the first derivative of the vertical motion function with respect to x, y' is the first derivative of the parabolic equation with respect to x, $\dot{v}$ and $\ddot{v}$ are the first derivative and second derivative of the vertical motion function with respect to time t respectively, μ is the structural damping, m is the self-weight per unit unstretched length.

The displacement $v(x,t)$ in Equation (7) can be written as

$$v(x,t)=f(x)q(t),p^*=f_1(x)p \tag{8}$$

where $f(x)=\sin(n\pi x/L)$ is the modal functions of the iced transmission line. Let n = 1, the single-mode discretization is adopted, and the research is mainly focused on the first-order mode. In addition, uniform distributed load (p^*) in vertical direction is considered, and $f_1(x)=1$ is the modal functions of external excitation, $q(t)$ is the time functions.

Based on Galerkin method, substituting equation (8) into equation (7) to obtain the nonlinear partial differential equation [25]:

$$\ddot{q}+\omega^2q+c_1q^2+c_2q^3+(\mu^*-c_3)\dot{q}+c_4\dot{q}^3=p\cos(\Omega t) \tag{9}$$

Equation (9) is the nonlinear galloping governing equation, which includes aerodynamic load and external excitation. The parameters in equation (9) are

$$\omega^2=\frac{1}{m}\frac{I_0}{I_m},c_1=12\frac{dES}{ml}\frac{I_1}{I_m},c_2=\frac{ES}{2ml}\frac{I_2}{I_m},\mu^*=\frac{\mu}{m},c_3=\frac{\tilde{a}}{m},c_4=\frac{\tilde{b}}{m}\frac{I_b}{I_m},p=\frac{p^*}{m}\frac{I_p}{I_m}; \tag{10}$$

where

$$I_0=H\int_0^l f'\bullet f\mathrm{d}x+64\frac{d^2ES}{l^5}(\int_0^l f\mathrm{d}x)^2,I_1=\int_0^l f'^2\mathrm{d}x\int_0^l f\mathrm{d}x,I_2=(\int_0^l f'^2\mathrm{d}x)^2,I_m=\int_0^l f^2\mathrm{d}x,I_b=\int_0^l f^4\mathrm{d}x,I_p=\int_0^l ff_1\mathrm{d}x \tag{11}$$

Equation (9) contains the first-order, and third-order nonlinear damping terms, the quadratic and cubic nonlinear restoring force term of q. The equation (9) can be regarded as the combined form of the Duffing equation and the Rayleigh equation [21].

3 Approximate Analytical Solution of Amplitude for Non-resonance

Equation (9) includes forced excitation term and Rayleigh damping term. When the amplitude (p) of excitation term is equal to 0, the system belongs to pure self-excited vibration; when the amplitude (p) of excitation term is greater than 0, the system belongs to forced-self-excited system. In order to discuss the adaptability of the approximate analytical solution of the multiple scale method to the forced-self-excited system, the multiple scale method is used in this section. Let the symbol of partial differential operator be:

$$\begin{aligned} \Omega t &= wT_0 + \varepsilon\sigma T_1 \\ DT &= D_0T_0 + \varepsilon(D_0T_1 + D_1T_0) \\ q &= q_0 + \varepsilon q_1 \end{aligned} \tag{12a-c}$$

If equation (9) is rewritten as a forced vibration far away from resonance, the galloping equation is as follows:

$$\ddot{q} + w^2 q + \varepsilon[c_1 q^2 + c_2 q^3 + (\mu^* - c_3)\dot{q} + c_4 \dot{q}^3] = p\cos(\Omega t) \tag{13}$$

Substituting equation (12) into equation (13), and $\Omega t = \xi T_0 + \varepsilon\sigma T_1$ in equation (13). And equating coefficients of like powers of ε^n (n=0,1) led to the following linear ordinary equations respectively [26]:

$$\begin{aligned} D_0^2 q_0 + w^2 q_0 &= p\cos(\xi T_0 + \varepsilon\sigma T_1) \\ D_0^2 q_1 + w^2 q_1 &= -[2D_0D_1q_0 + c_1 q_0^{\,2} + c_2 q_0^{\,3} + (\mu + c_3)D_0 q_0 + c_4 (D_0 q_0)^3] \end{aligned} \tag{14a-b}$$

where D_k represents the partial derivative of T_k, the solutions of equation(14a) can be written in this form:

$$q_0 = A(T_0, T_1)e^{iwT_0} + \overline{A}(T_0, T_1)e^{-iwT_0} + Be^{i\Omega T_0} + \overline{B}e^{-i\Omega T_0} \tag{15}$$

where A and B can be set as:

$$\begin{aligned} A(T_0, T_1) &= 1/2a(T_0, T_1)\exp[i\beta(T_0, T_1)] \\ B &= P/[2|w^2 - \Omega^2|] \end{aligned} \tag{16a-b}$$

Substituting equation (15) into equation (14b) to obtain:

$$\begin{aligned} &D_0^2 q_1 + w^2 q_1 = -2iwD_1(Ae^{iwt} + Be^{i\Omega t}) - c_1[A^2e^{2iwt} + A\overline{A} + B\overline{B} + 2ABe^{2i(w+\Omega)t} + 2A\overline{B}e^{2i(w-\Omega)t} + B^2e^{2i\Omega t}] \\ &-c_2[A^3e^{3iwt} + B^3e^{3i\Omega t} + 6AB\overline{B}e^{iwt} + 6A\overline{A}Be^{i\Omega t} + 3A^2\overline{A}e^{iwt} + 3A^2Be^{i(2w+\Omega)t} + 3B^2\overline{B}e^{i\Omega t} + 3AB^2e^{i(w+2\Omega)t} \\ &+3\overline{A}^2Be^{i(\Omega-2w)t} + 3B^2\overline{A}e^{i(2\Omega-w)t}] - (\mu + c_3)(iwAe^{iwt} + i\Omega Be^{i\Omega t}) - c_4[6iw^2A\overline{A}Be^{i\Omega t} - iw^3A^3e^{3iwt} - i\Omega^3B^3e^{3i\Omega t} \\ &+3iw^3A^2\overline{A}e^{iwt} + 6iw\Omega^2AB\overline{B}e^{iwt} + 3i\Omega^3B^2\overline{B}e^{i\Omega t} - 3i\Omega w^2A^2Be^{i(2w+\Omega)t} - 3iw\Omega^2B^2Ae^{i(2\Omega+w)t} \\ &-3iw\Omega^2A\overline{B}^2e^{i(w-2\Omega)t} - 3i\Omega w^2B\overline{A}^2e^{i(\Omega-2w)t}] + cc \end{aligned} \tag{17}$$

In equation (17), if the frequency(Ω) of external excitation term satisfies these condition: $\Omega \neq \omega + \varepsilon\sigma_1; \Omega \neq 2\omega + \varepsilon\sigma, \Omega \neq 3\omega + \varepsilon\sigma, \Omega \neq \omega/2 + \varepsilon\sigma, \Omega \neq \omega/3 + \varepsilon\sigma$, then the equation (17) will generate the corresponding duration term. Therefore, the harmonic resonance of the system is easy to be excited.

In order to prevent the generation of super-harmonic resonance and sub-harmonic resonance, let excitation frequency Ω=*w*/4. And combine equation (16-17) to obtain the averaging equation about amplitude and phase of the system [27]:

$$\begin{aligned}\dot{a} &= -(\mu + c_3)a/2 - 3w^2 c_4 a^3/8 - 3c_4\Omega^2 B^2 a \\ a\dot{\beta} &= 3c_2 a^3/8w + 3c_2 B^2 a/w\end{aligned} \tag{18a-b}$$

After integrating equation (18) over time(*t*), it can be obtained that:

$$\begin{aligned}a &= \sqrt{1/[(1/a_0{}^2 + n/m)e^{-2mt} - n/m]} \\ \beta_2 &= \beta_0 + [3c_2 a^2/8w + 64c_2 P^2/75w^5]t\end{aligned} \tag{19a-b}$$

In equation (19), the *a*(t) is amplitude function, where *m* and *n* depend on the physical structure parameters and aerodynamic parameters of the iced transmission line, and *m* determines the variation trend of amplitude.

When the excitation amplitude (*p*) is less than the critical value, there is self-excited vibration in the forced-self-excited system, that is, the necessary and sufficient conditions for the existence of self-excited vibration are as follows:

$$a_0 < \lim_{t\to\infty}\sqrt{1/[(1/a_0{}^2 + n/m)e^{-2mt} - n/m]} = C \tag{20}$$

If the parameter $m > 0$ is satisfied, then equation (19a) is convergent, and the excitation amplitude (*p*) satisfies the condition of equation (20). Then the system can still form self-excited vibration without destroying the condition of self-excited vibration, and the steady-state motion of the system is composed of the self-excited vibration and the forced vibration.

When the external excitation is relatively strong, $m < 0$, that is to say, the condition of destroying self-excited vibration is as follows:

$$\lim_{t\to\infty}\sqrt{1/[(1/a_0{}^2 + n/m)e^{-2mt} - n/m]} = 0 \tag{21}$$

If the excitation amplitude does not satisfy the condition of equation (20), the amplitude of self-excited vibration tends to zero with time. If the excitation amplitude meets the condition of equation (21), the self-excited vibration can not be formed, which indicates that there is no self-excited vibration in the forced-self-excited system. The parameters in equation (19a), equation (20), and equation (21) are as follows:

$$m = -(\mu + c_3)/2 - 3c_4\Omega^2 B^2; n = -3w^2 c_4/8 \tag{22}$$

In order to avoid the principal resonance and intense harmonic resonance, let Ω = *w*/4, the amplitude expression is obtained by combining equation (12b-c), equation (15-17), and equation (19)：

$$
\begin{aligned}
q^* = {} & a\bullet\cos\psi + 2B\bullet\cos(\frac{\psi}{4}) + \varepsilon[-(\frac{32c_2a^2B}{10w^2} + \frac{32c_2B^3}{5w^2})\bullet\cos(\frac{\psi}{4}) + (\frac{4c_4wa^2B}{5} + \frac{c_4wB^3}{5} + \frac{8uB}{15w})\bullet\sin(\frac{\psi}{4}) \\
& - \frac{c_4wB^2a}{4}\bullet\sin(\frac{\psi}{2}) - (\frac{4c_2\bar{B}^2a}{w^2} + \frac{8c_1B^2}{3w^2})\cos(\frac{\psi}{2}) + \frac{12c_2B^2a}{5w^2}\bullet\cos(\frac{3\psi}{2}) + \frac{3c_4wB^2a}{20}\bullet\sin(\frac{3\psi}{2}) - \frac{wc_4B^3}{14}\bullet\sin(\frac{3\psi}{4}) \\
& - (\frac{32c_1B_1a}{7w^2} + \frac{32c_2B^3}{7w^2})\bullet\cos(\frac{3\psi}{4}) + \frac{32c_2Ba}{9w^2}\bullet\cos(\frac{5\psi}{4}) + \frac{8c_2\bar{B}a^2}{11w^2}\bullet\cos(\frac{7\psi}{4}) + \frac{2wc_4\bar{B}a^2}{11}\bullet\sin(\frac{7\psi}{4}) \\
& + \frac{24c_2Ba^2}{65w^2}\bullet\cos(\frac{9\psi}{4}) + \frac{6wc_4Ba^2}{65}\bullet\sin(\frac{9\psi}{4}) + \frac{c_1a^2}{6w^2}\bullet\cos(2\psi) + \frac{c_2a^2}{32w^2}\bullet\cos(3\psi) \\
& + \frac{wc_4a^3}{32}\bullet\sin(3\psi) - (\frac{a^2}{2} + 2B\bar{B})\frac{c_1}{w^2}]
\end{aligned}
\tag{23}
$$

where the ψ is:

$$
\psi = wt + \beta_2 \tag{24}
$$

According to on-site observations, the icing of crescent-shaped is a common ice type with galloping. In addition, the parameters of iced transmission can be obtained by experiment. In order to facilitate analysis and comparison, as shown in Tab.1, citing the geometrical parameters, material parameters and related aerodynamic parameters in the reference [28]:

Tab.1 The physical parameters of transmission line

parameter	symbol	units	value
tension	H	N	30 000
span	L	m	125.88
Young's modulus	E	N/mm^2	47 803.3
diameter	D	m	0.0286
mass per unit length	m	Kg/m	2.379
traverse area	S	mm^2	423.24
air mass density	ρ	Kg/m^3	1.2929
wind velocity	U	m/s	4.0
sag	d	m	1.5432
vertical dumping	μ	/	0.0005
aerodynamic parameters	A'	/	-0.1667
aerodynamic parameters	B'	/	8.3581

Fig. 3(a-d) is the time history displacement diagram of forced-self-excited system, and the partial curve of the time history displacement diagram from 2000 to 2020 s. The solid line represents the numerical solution, which is obtained by solving equation (9) with Runge Kutta function in MATLAB; the dotted line represents the approximate analytical solution of the multiple scale method, which corresponds to equation (23). When the amplitude (p) of the excitation term in Fig. 3(a) is equal to 0, the system belongs to self-excited vibration; when the amplitude (p) of the excitation term in Fig. 3(b-d) is greater than 0, the system belongs to forced-self-excited vibration.

In Fig. 3(a), the excitation amplitude p=0 in equation (9), and the time history displacement diagram belongs to pure self-excited vibration. Under the effect of Rayleigh damping, the response amplitude of the system gradually increases from 0.010 m to 0.201 m, and in this process, the vibration velocity of the system also increases. From the comparison of time history displacement

curves, it can be seen that the numerical solution is in good agreement with the approximate analytical solution of the multiple scale method, and the error between amplitudes is only 0.70%. As shown in Fig. 3(b), the excitation amplitude p=0.5, and the self-excited vibration characteristics of the time history displacement diagram had changed. Under the action of external excitation, the initial vibration amplitude of the system increases from 0.010 m to 0.100 m. The response amplitude of the system increases from 0.201 m to 0.235 m, and the galloping time (the time required for galloping of iced transmission line system under initial disturbance) is shortened from 1 750 s to 1 050 s. Moreover, and the form of time history displacement diagram also changes from the simple harmonic vibration to irregular vibration. When the excitation amplitude p=5 and p=8, the time history displacement diagram is shown in Fig. 3(c) and 3(d), and the vibration amplitude increases from 0.201 m to 0.536 m, and 0.929 m. With the increases in excitation amplitude (p), and the self-excited vibration characteristics of forced-self-excited system disappear gradually.

In addition, with the increase in the excitation amplitude (p), the error between the approximate analytical solution and the numerical solution increases gradually. When the excitation amplitude p=0.5, the error should be 1.51% in Fig. 3(b); when the excitation amplitude p=8, the error should be 14.142% in Fig. 3(d). And the numerical solution does not agree with the approximate analytical solution of the multiple scale method in the contrast curve of time history displacement diagram. With the increase of the excitation amplitude (p), the forced-self-excited system from the weak nonlinear system to the strong nonlinear system, and the error of the approximate analytical solution of the multiple scale method increases.

Fig. 3(b-d) shows the time history displacement curve of iced transmission line under periodic excitation. When the excitation amplitude p=0.5 and p=5, the system satisfies the discriminant equation (20), and the vibration form of the forced-self-excited system is the superposition form of self-excited vibration and forced vibration. In Fig. 3(d), when the excitation amplitude is greater than the critical value, the self-excited vibration condition of the forced self-excited system is destroyed. When the excitation amplitude p=8, the forced-self-excited system satisfies discriminant formula (21), and the vibration form is the forced vibration regulated by Rayleigh damping.

Fig. 3(e) is obtained by using Maple software to draw the amplitude analytical solution equation (19a), and the equation (19a) only represents the stable amplitude of self-excited vibration in forced self-excited system. The curves b, c, and d in Fig. 3 are obtained by substituting the excitation amplitudes p = 0.5, 5, and 8 into equation (19a), and the curves also correspond to the excitation amplitudes in Fig.3(b), 3(c), and 3(d) respectively. The increase of excitation amplitude (p) makes the effect of self-excited vibration in forced-self-excited system smaller and smaller. The curves b and curves c in Fig. 3(e) are in the range of discriminant formula (20), and the curve d is in the range of discriminant formula (21). As the excitation amplitude p=0.5 increases to p=5, the response

amplitude of self-excited vibration decreases from the point a_b to the point a_c; when the excitation amplitude p=8.0, the response amplitude of self-excited vibration tends to be close to 0, which also verifies the correctness of discriminant formula (20) and (21).

After the above analysis on Figure 3, it is easy to get that: with the increase in excitation amplitude (p), the vibration form of forced-self-excited system has gone through three stages.

(1), In Fig. 3(a), the excitation amplitude (p) is equal to 0, and the vibration form of the system is the pure self-excited vibration.

(2), In Fig. 3(b) and 3(c), the excitation amplitude (p) satisfies the discriminant formula (20), and the vibration form of the system is the superposition form of self-excited vibration and forced vibration.

(3), In Fig. 3(d), the excitation amplitude (p) satisfies the discriminant formula (21), and the vibration form of the system is forced vibration regulated by Rayleigh damping.

In forced-self-excited system, the self-excited vibration condition of iced transmission line under wind load excitation is destroyed by forced excitation, which is called quenching phenomenon.

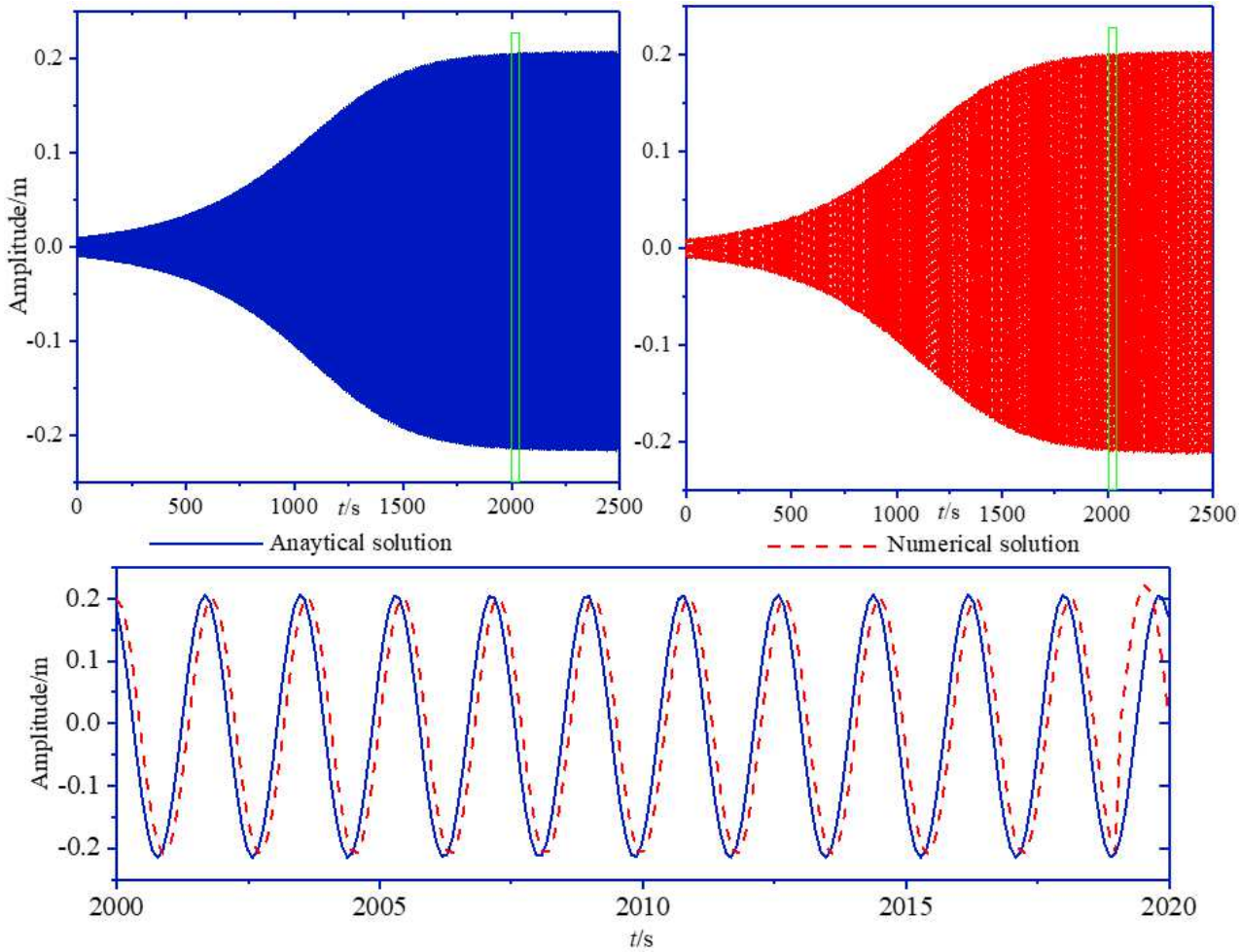

(a) Excitation amplitude p=0

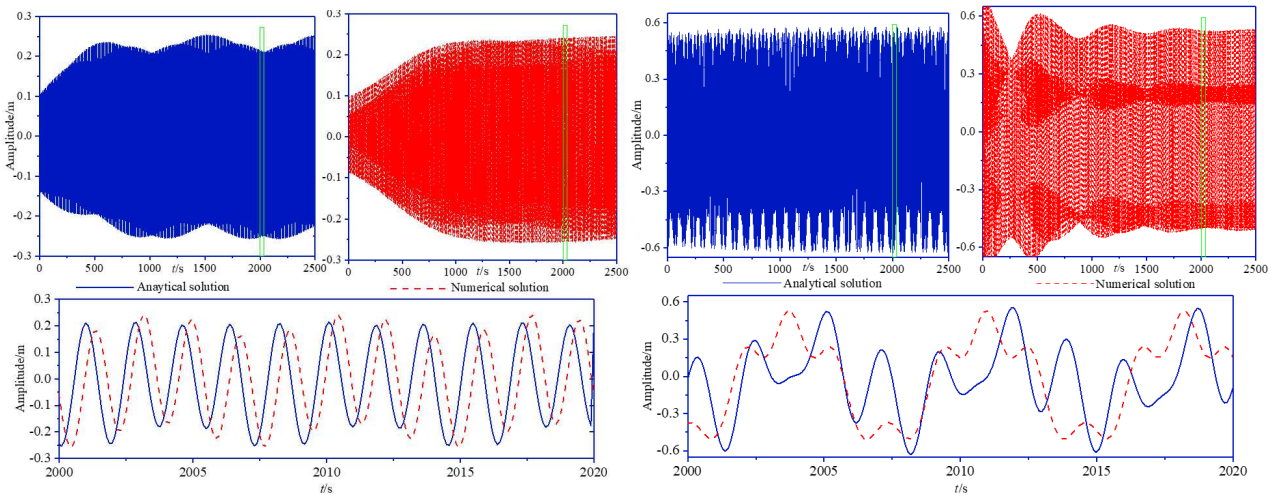

(b) Excitation amplitude p=0.5 (c) Excitation amplitude p=5.0

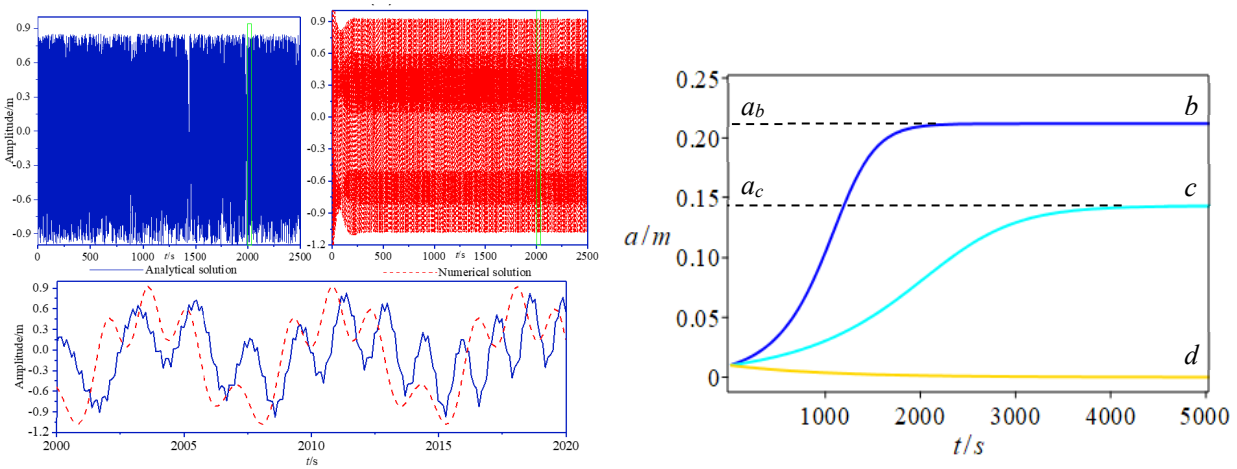

(d) Excitation amplitude p=8.0 (e) The amplitude curve of self-excited vibration

Fig.3 The time history displacement diagram of forced-self-excited system

4 Approximate Analytical Solution of Weakly Nonlinear System

This section discusses the principal resonance of forced-self-excited system, which the excitation frequency Ω is equal to the natural frequency ω. It is generally considered that the damping and nonlinear terms have little effect on the system. To this end, the form of the solution of equation (9) is rewritten as follows:

$$\ddot{q}+w^2q+\varepsilon[c_1q^2+c_2q^3+(\mu^*-c_3)\dot{q}+c_4\dot{q}^3]=\varepsilon p\cos(\Omega t) \tag{25}$$

Substituting equation (12) into equation (25), and $\Omega t=\xi T_0+\varepsilon\sigma T_1$ in equation (25). And equating coefficients of like powers of ε^n (n=0,1) led to the following linear ordinary equations respectively:

$$\begin{aligned} &D_0^2q_0+w^2q_0=0 \\ &D_0^2q_1+w^2q_1=-[D_0{}^2q_1+2D_0D_1q_0+c_1q_0{}^2+c_2q_0{}^3+(\mu+c_3)D_0q_0+c_4(D_0q_0)^3-p\cos(\Omega t)] \end{aligned} \tag{26a-b}$$

where D_k represents the partial derivative of T_k, the solutions of equation (26a) can be written in this form:

$$q_0=\Lambda(T_1)e^{iwT_0}+\bar{\Lambda}(T_1)e^{-iwT_0} \tag{27}$$

where Λ can be set as:

$$\Lambda(T_1)=1/2a(T_1)\exp[i\hat{\beta}(T_1)] \tag{28}$$

Substituting equation (17-a) and equation (28) into equation (26b), it can be obtained:

$$D_1\Lambda=\frac{3ic_2}{2w}\Lambda^2\overline{\Lambda}-\frac{3c_4}{2}w^2\Lambda^2\overline{\Lambda}-\frac{\mu+c_3}{2}\Lambda-\frac{ip}{4w}e^{i\sigma T_1} \tag{29}$$

Combining equation (28), equation (29) to obtain the averaging equation about amplitude and phase of the system [29]:

$$\begin{aligned}\dot{a}&=\frac{-(\mu+c_3)}{2}a-\frac{3}{8}c_4w^2a^3+\frac{p}{2w}\sin(\sigma T_1-\hat{\beta})\\ a\dot{\hat{\beta}}&=\frac{3c_2}{8w}a^3-\frac{p}{2w}\cos(\sigma T_1-\hat{\beta})\end{aligned} \tag{30a-b}$$

Introducing $\gamma=\sigma T_1-\beta$, in order to acquire the steady-state solution of the amplitude and phase of equation (30), let $D_1A=0$, and obtain the amplitude-frequency equation by eliminating γ:

$$\frac{p^2}{4w^2a^2}=(\sigma+\frac{3c_2a^2}{8w})^2+(\frac{\mu+c_3}{2}+\frac{3w^2c_4a^2}{8})^2 \tag{31}$$

For the forced-self-excited system close to the principal resonance, the analytical expression (31) of amplitude frequency response relation under weak excitation is obtained by using the multiple scale method. In order to verify the correctness of the analytical solution equation (31), the excitation frequency Ω is equal to the natural frequency w of the forced-self-excited system, and the tuning parameter σ=0. As shown in Fig. 4, the curve of excitation amplitude and response amplitude of equation (31) is drawn with mathematical software maple. The excitation amplitudes p^* =3.736, 7.472, 11.208, 14.944, and 18.680 N/m are transformed by equation (10) and equation (11), respectively corresponding to the excitation amplitudes p= 2, 4, 6, 8, and 10 in the abscissa of Fig. 4. By substituting the excitation amplitude into equation (9), the points a_i、b_i、c_i、d_i in Fig. 4 (i=1, 2, 3, 4, 5) in Fig. 4 are obtained by using MATLAB. These points all correspond to the response amplitude (positive) of the time history displacement diagram.

As shown in Fig. 4(a), when the wind velocity is U=4m/s, the numerical solution obtained by MATLAB is in good agreement with the force-amplitude curve obtained by multiple scale method; however, when the response amplitude is greater than 2, the error between the numerical solution and the force-amplitude curve increases from 2.98% of p=6 to 5.42% of p=10. Therefore, when the response amplitude is greater than 2 and the excitation amplitude continues to increase, the error of analytical solution will increase, but the force-amplitude curve can still be analyzed. It can also be seen from Fig. 4(a) and Fig. 4(b) that when the wind velocity changes from 4 m/s to 8 m/s, the error between the analytical solution and the numerical solution of the force-amplitude response increases; it also shows that the increase of wind velocity also enhances the nonlinearity of the system.

In Fig. 4(c), when Young's modulus E=9 560.7, 47 803.3 N/mm^2, the force-amplitude curve is compared. When Young's modulus E=9 560.7 N/mm^2, the numerical solution obtained by MATLAB

is in good agreement with the force-amplitude curve obtained by multiple scale method. When Young's modulus E=47 803.3 N/mm^2, the error between the analytical solution and the numerical solution obtained by the multiple scale method increases obviously. The analytical solution of multiple scale method is only suitable for weakly nonlinear systems. With the increase of Young's modulus, the stiffness and nonlinearity of the system increase gradually, which makes the error of the approximate analytical solution of multiple scale method increase. In addition, the increase of the Young's modulus reduces the response amplitude of the forced-self-excited system, indicating that the increase of the Young's modulus is also conducive to reducing the vibration amplitude of the iced transmission line.

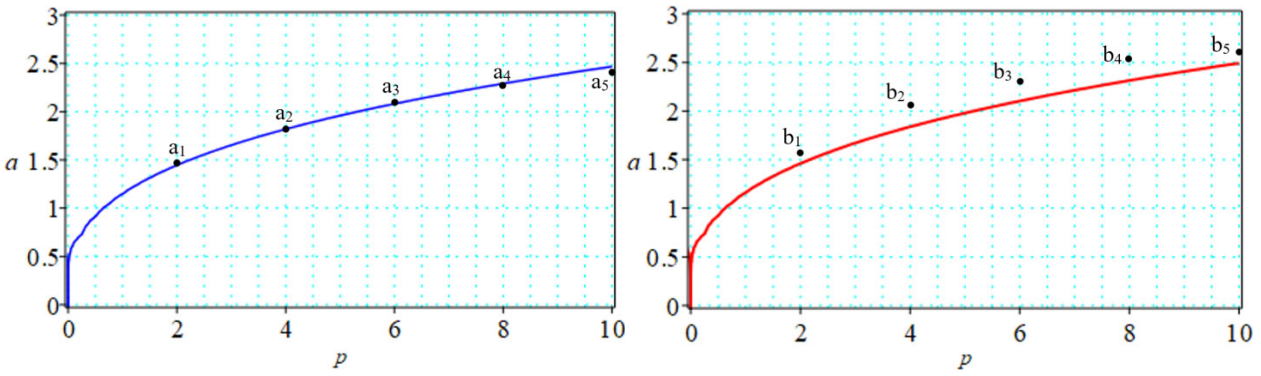

(a) U=4 m/s, H=30 000 N (b) U=8 m/s, H=30 000 N

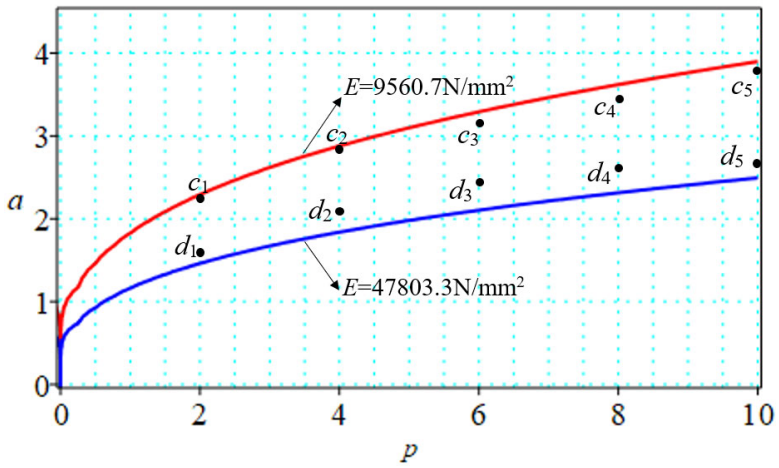

(c) U=8 m/s, H=30 000 N

Fig.4 The excitation amplitude(p)-response amplitude(a) curve

5 Numerical Solution of Strongly Nonlinear System

In Section 3, the multiple scale method is used to solve the forced-self-excited system, and the approximate analytical solution of the system is obtained; in Section 4, the expression of the

amplitude frequency response relation of the forced-self-excited system is obtained by using the multiple scale method. With the increase in wind velocity and excitation amplitude, the nonlinearity of the system is enhanced, and the error of analytical solution of the multiple scales method is increased. Therefore, in order to analyze the dynamic response of forced-self-excited system more accurately, section 5 uses the Runge Kutta function of MATLAB.

In order to analyze the influence of excitation amplitude and frequency on the dynamic response of forced-self-excited system, the Runge Kutta function in MATLAB is used to solve the equation (9) directly, and the time history displacement diagram and phase trajectory diagram (q_0=0.01 m, U=4 m/s) in Fig. 5-11 are obtained. In addition, the nonlinear dynamic phenomena of principal resonance, super-harmonic resonance and sub-harmonic resonance are analyzed.

5.1 Numerical Solution of Principal Resonance

Under the condition of external excitation, when the frequency of external excitation is equal to the natural frequency of the system, the system is prone to resonance, which is called the principal resonance.

When the excitation amplitude (p) is equal to 0, the system only has self-excited vibration, not forced vibration. As time goes on, the energy input to the system increases. When the energy dissipated by viscous damping is equal to the energy input to the system, the system reaches a stable state. When the self-excited vibration is stable, the frequency and amplitude of the time history displacement image are constant, so a stable limit cycle is formed. Because of the influence of the curvature of the iced transmission line, the response amplitude in the negative direction is greater than that in the positive direction, which means that the vibration center of system drifts. In Fig. 5(a), the area ($a<0$) indicates that the iced transmission line is above the equilibrium position directly, and the iced transmission line is under the combined action of gravitational potential energy, inertia, and elastic potential energy; the area ($a>0$) indicates that the iced transmission line is below the equilibrium position directly, and the elastic potential energy and inertia of the iced transmission line have to overcome the gravitational potential energy of iced transmission line. Therefore, the vibration center of the system is not in equilibrium.

In Fig. 5(a), as the excitation amplitude p=0, it can be seen that the galloping time(t) of the history displacement curves is 2 000 s; the peak values of galloping amplitude (maximum stable amplitude of iced transmission line under external excitation) and galloping velocity (maximum stable vibration velocity of iced transmission line under external excitation) also increase to -0.211 m and 0.714 m/s; the limit cycle of the stable system is a closed elliptic cycle, at this time, the system forms the classic galloping phenomenon of transmission line. In Fig. 5(b), as the excitation amplitude p=0.1, it can be seen that the galloping time(t) of the history displacement curves is 120 s. Therefore,

under the condition of external excitation, the galloping time(t) is shortened from 2 000 s of p=0 to 120 s of p=0.1; in addition, the peak values of galloping amplitude and galloping velocity are also increased to -0.607 m and 1.986 m/s. In Fig. 5(c), as the excitation amplitude p=2.5, the galloping time(t) of the history displacement curves is 10 s, and the peak values of galloping amplitude and galloping velocity increase to -2.128 m and 6.304 m/s. Through the analysis of Fig. 5, it can be concluded that the principal resonance response of forced-self-excited system is very intense. Under the condition of external excitation, the galloping time of the system shortens sharply, and the galloping amplitude and galloping velocity increase rapidly.

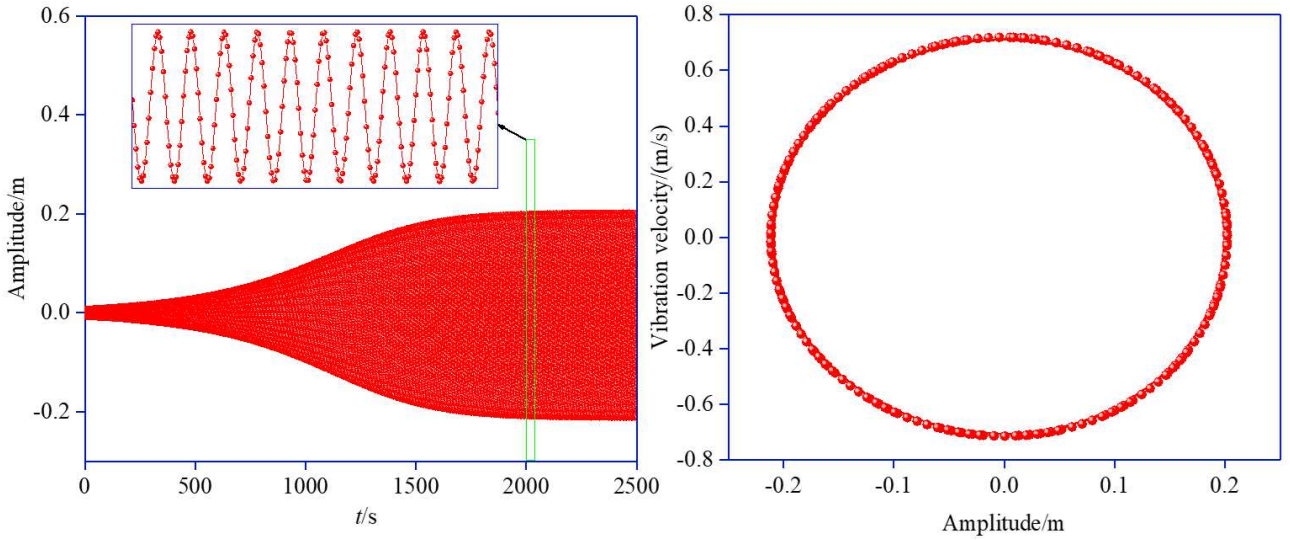

(a) Excitation amplitude p=0

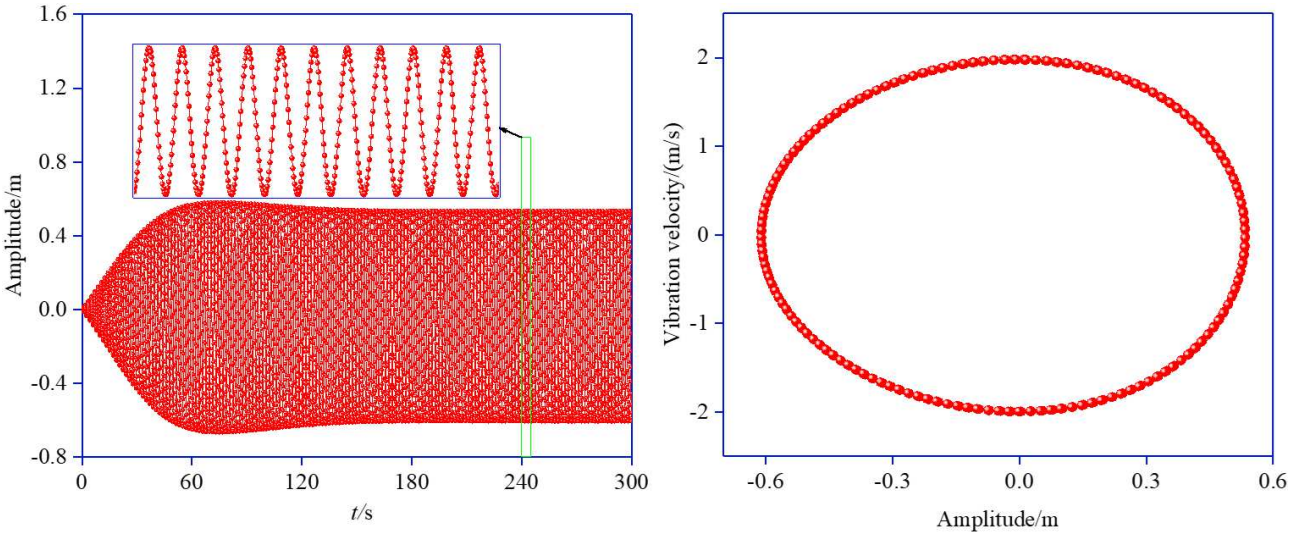

(b) Excitation amplitude p=0.1

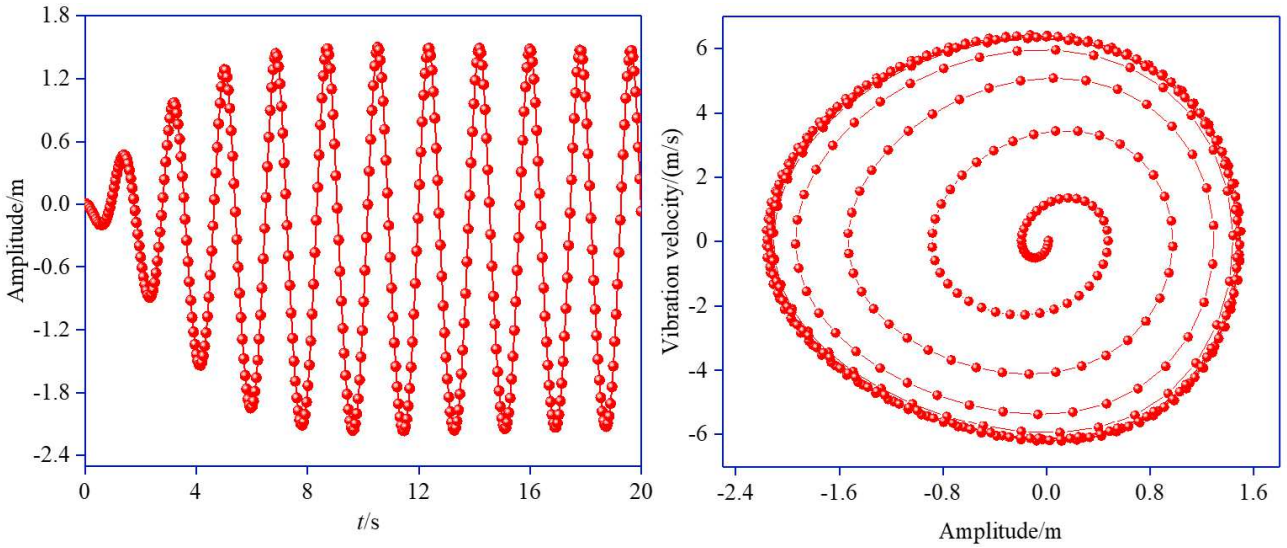

(c) Excitation amplitude p=2.5

Fig. 5 The time history displacement curve and phase diagram

5.2 Numerical Solution of 2-order Super-harmonic Resonance

When the frequency of the external excitation is equal to half of the natural frequency of the system, the resonance of the system is called 2-order super-harmonic resonance.

When the excitation amplitude p=0.4, it can be seen from Fig. 6(a) that the galloping time(t) of the history displacement curves is 1 200 s; the peak values of galloping amplitude and galloping velocity also increase to 0.235 m, -0.741 m/s; the phase diagram under 2-order super-harmonic excitation is an elliptic ring with period-two periodic motion. When the excitation amplitude p=2, it can be seen from Fig. 6(b) that the system still maintains the form of period-two periodic motion; the galloping time(t) of the history displacement curves is 60 s; and the peak value of galloping amplitude and galloping velocity also increases to 0.688 m and 2.192 m/s. As the excitation amplitude increases to p=12, it can be seen from Fig. 6(c) that the galloping time is t=30 s; the peak values of galloping amplitude and galloping velocity increase to -3.411 m and 7.685 m/s; at this time, the system still maintains the form of period-two periodic motion. As the excitation amplitude increases to p=112, it can be seen from Fig. 6(d) that the galloping time is t=0 s; however, the phase diagram changes from period-two periodic motion to period-three periodic motion.

Under the condition of 2-order super-harmonic excitation, in Fig. 6(a), the phase diagram increases a period of vibration in the region above the equilibrium position. As shown in Fig. 6, with the increasing of excitation amplitude, from Fig. 6(a) to Fig. 6(b), and then to Fig. 6(c), the galloping amplitude of limit cycle in outer ring increases faster than that in inner ring, and the increasing trend is more obvious in the region of amplitude less than 0. It is worth noting that with the increase of excitation amplitude, the phase diagram can change from the form of period-two periodic motion to that of period-three periodic motion in Fig. 6(d).

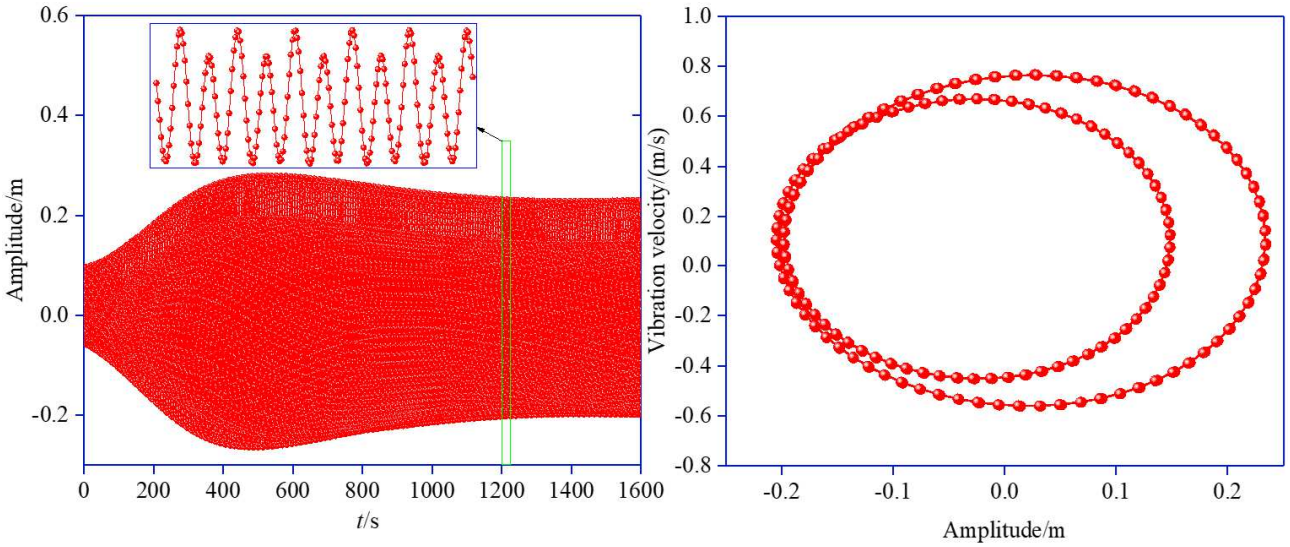

(a) Excitation amplitude p=0.4

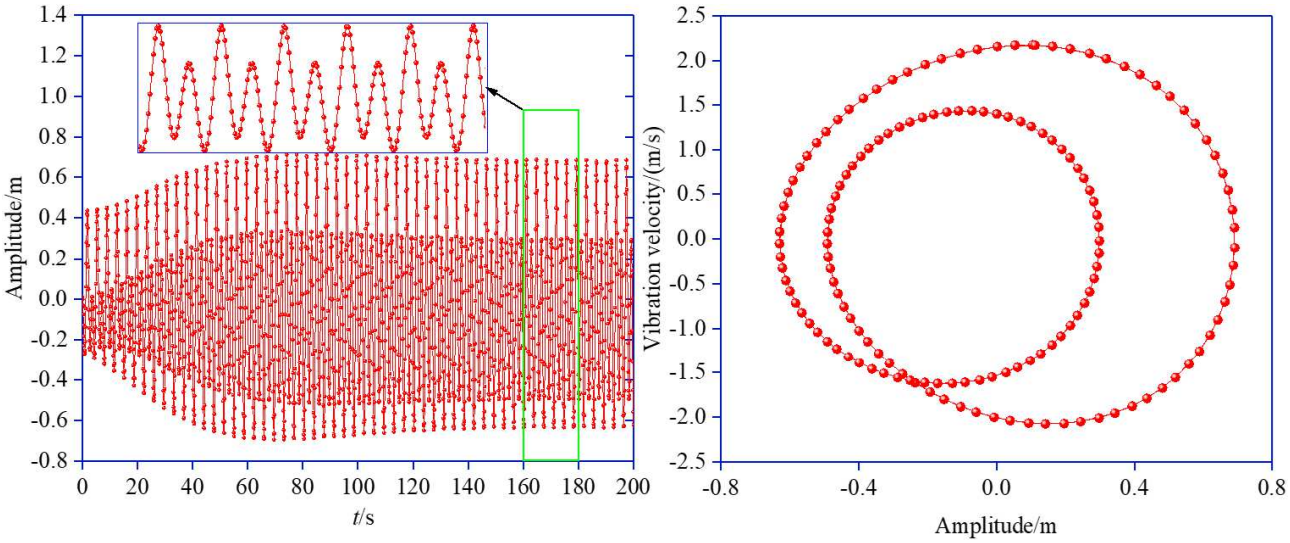

(b) Excitation amplitude p=2

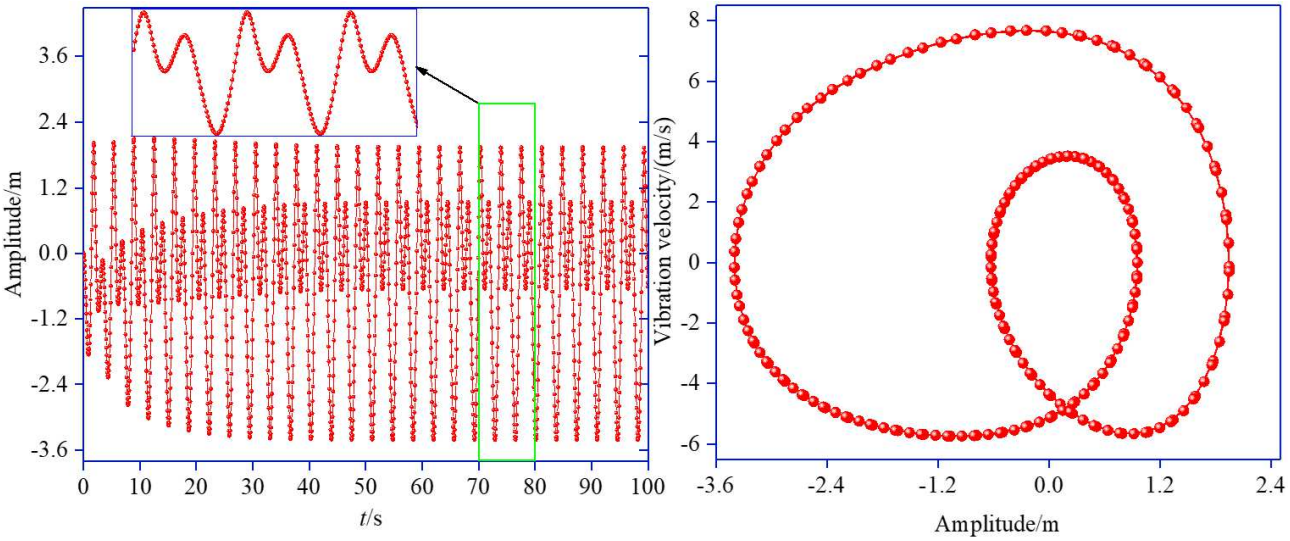

(c) Excitation amplitude p=12

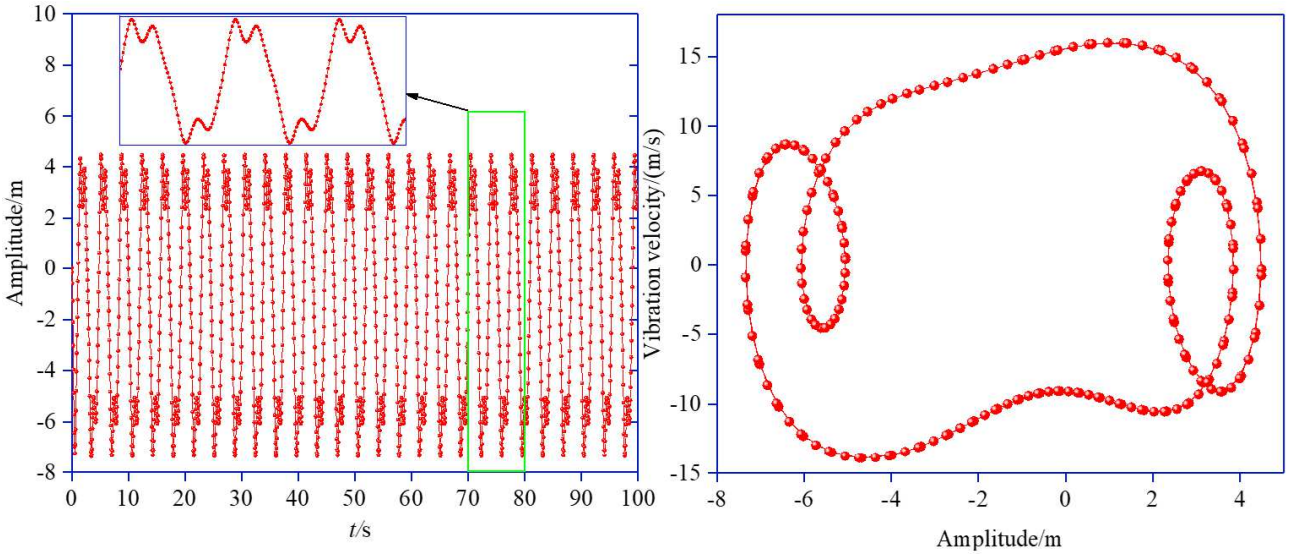

(d) Excitation amplitude p=122

Fig. 6 The time history displacement curve and phase diagram

5.3 Numerical Solution of 3-order Super-harmonic Resonance

When the frequency of the periodic excitation is equal to one third of the natural frequency of the system, the resonance response of the system is called 3-order super-harmonic resonance.

As the excitation amplitude p=1, it can be seen from Fig. 7(a) that the phase diagram adds a period of vibration to the upper and lower sides of the equilibrium position, and the system behaves as an elliptic ring with period-three periodic motion. The galloping amplitude and galloping velocity of the time history displacement curve is -0.309 m, 0.811 m/s in Fig. 7(a). When the excitation amplitude p=2, it can be seen from Fig. 7(b) that at this time, the system also maintains the form of period-three periodic motion; however, the time history displacement curve of the system does not have the characteristics of self-excited vibration. In Fig. 7(c) and Fig. 7(d), when the excitation amplitude increases to p=10 and p=15, it can be seen that the galloping amplitude and galloping velocity continued to increase, and the galloping time of history displacement curve continued to shorten; at this time, the system still maintains the form of period-three periodic motion, which is different from Fig. 7(a) and Fig. 7(b).

As shown in Fig. 7, with the increasing of excitation amplitude, from Fig. 7(a) to Fig. 7(b), then to Fig. 7(c), and to Fig. 7(d), the vibration center of the inner ring shifts from the region near the equilibrium position to the region above the equilibrium position and to the region below the equilibrium position, respectively. However, with the increase of the excitation amplitude, the vibration center of the inner ring shifts from the region above the equilibrium position to the region below the equilibrium position gradually. When the excitation amplitude p = 15, the phase diagram of Fig. 7 (d) is formed. In Fig. 7, it is worth noting that, even if the excitation amplitude increases continuously, the phase diagram always keeps the vibration form of period-three periodic motion.

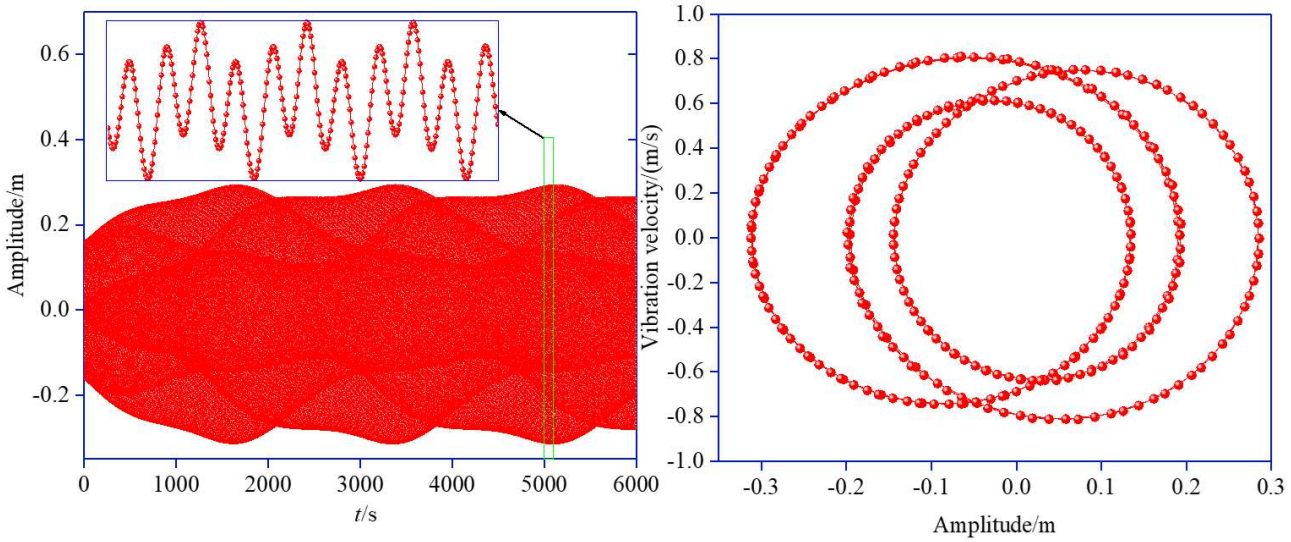

(a) Excitation amplitude p=1

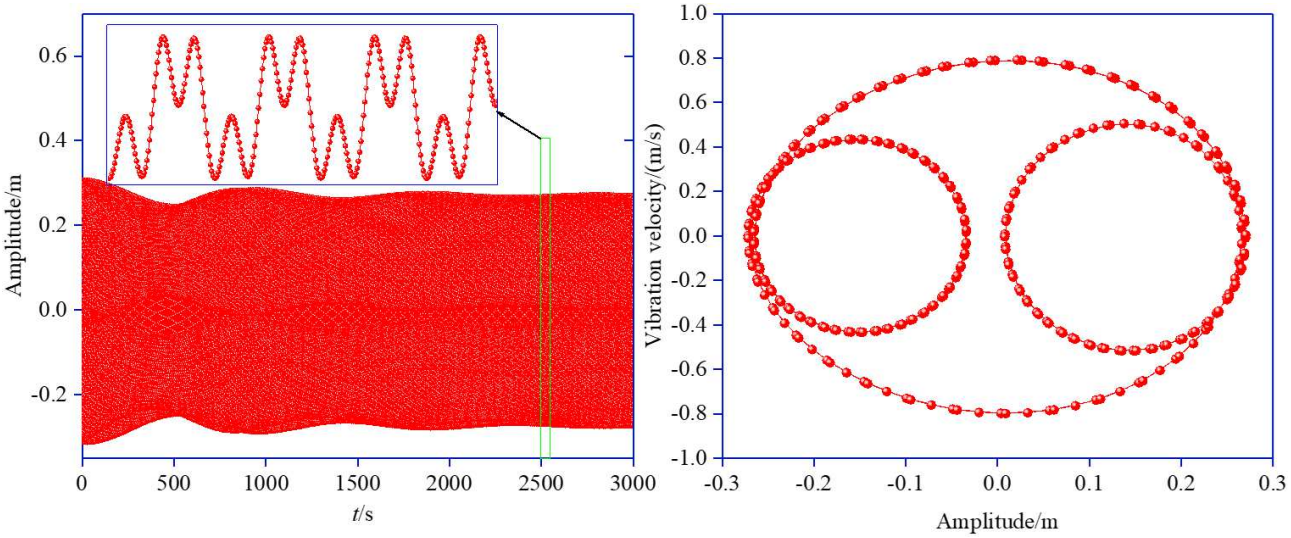

(b) Excitation amplitude p=2

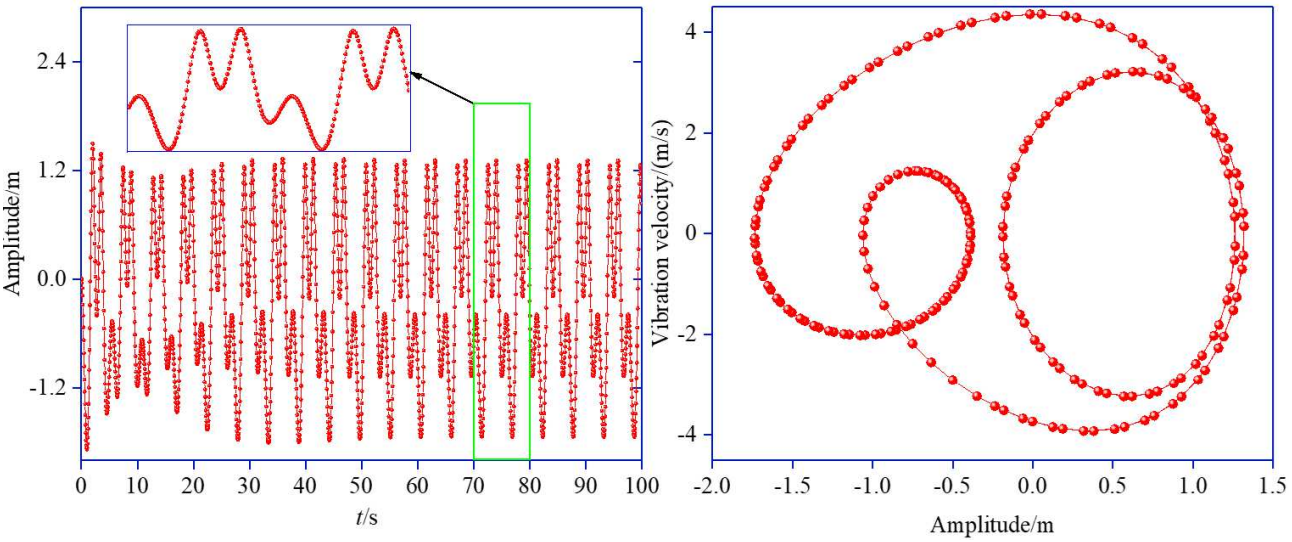

(c) Excitation amplitude p=10

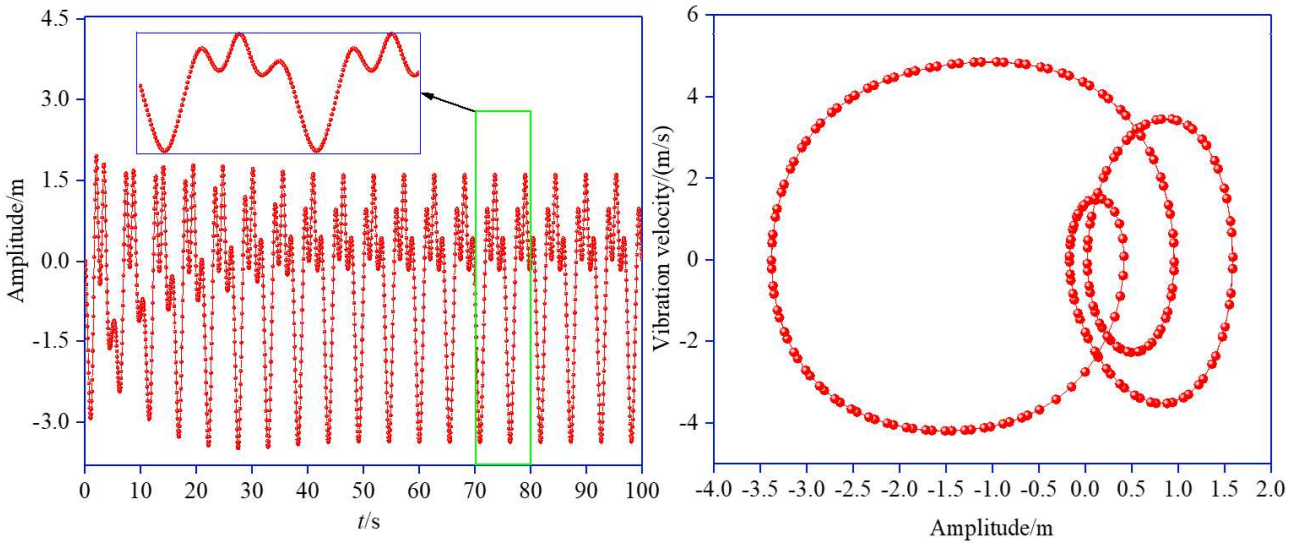

(d) Excitation amplitude p=15

Fig. 7 The time history displacement curve and phase diagram

In order to show the trajectory of the phase diagram more clearly, the phase diagrams in Fig. 8 and Fig. 11 are drawn as scatter diagrams. Under the condition of the 3-order super-harmonic excitation, Fig. 8 shows the time history displacement image and phase diagram of the forced self-excited system with different excitation amplitudes (p). As shown in Fig.8(a), the left figure shows the time history displacement diagram of the system when the excitation amplitude p=0.5, and the right figure shows the phase diagram of the rectangular frame part of the dotted line in the left figure. The phase diagram of Fig. 8(b) corresponds to the time period (3 000-3 800 s) of Fig. 7(a); the phase diagram of Fig. 8(c) corresponds to the time period (0-2 000 s) of Fig. 7(b).

As shown in Fig. 8(a), when the excitation amplitude is small (p=0.5), the vibration form of the system is the superposition of forced vibration and self-excited vibration, in which the self-excited vibration part is that the system forms a stable cyclic vibration after a period of time under the action of initial excitation and external excitation. And the forced vibration part is the beat vibration form of the system under external excitation.

In Fig. 8, from Fig. 8(a) to Fig. 8(b), and then to Fig. 8(c), the external excitation effect in the system is enhanced, and the phase diagram change from the form of period-one periodic motion to that of period-three periodic motion gradually. In 8(c), with the increase in excitation amplitude (p), the characteristics of self-excited vibration disappear gradually, and finally form the quasi-periodic vibration with period-three periodic motion.

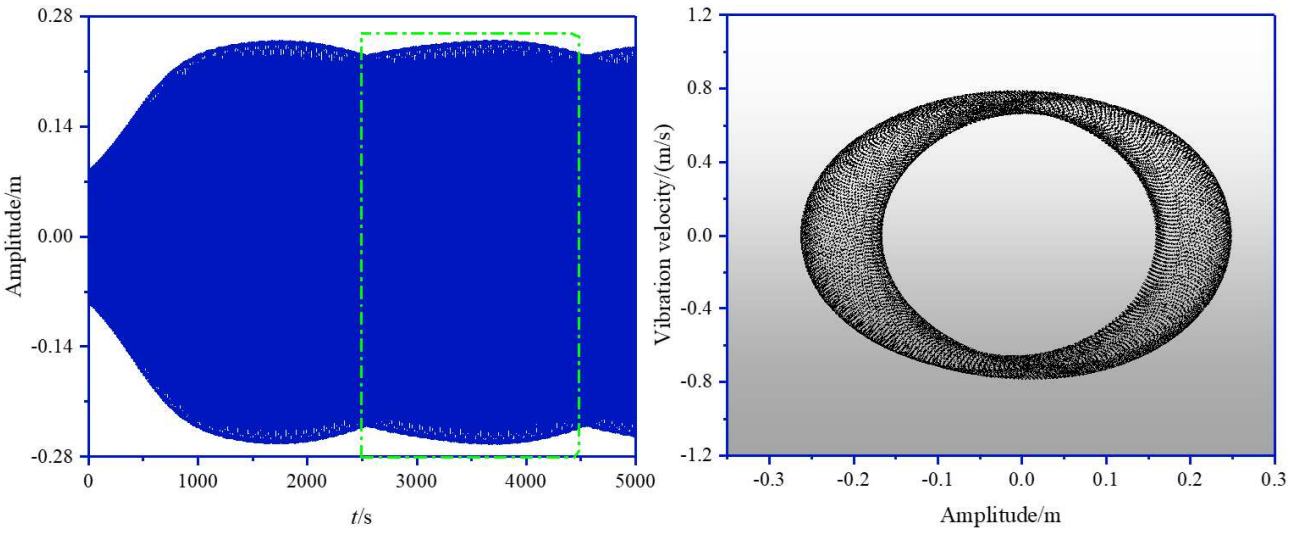

(a) Excitation amplitude p=0.5(2 500 -4 500 s)

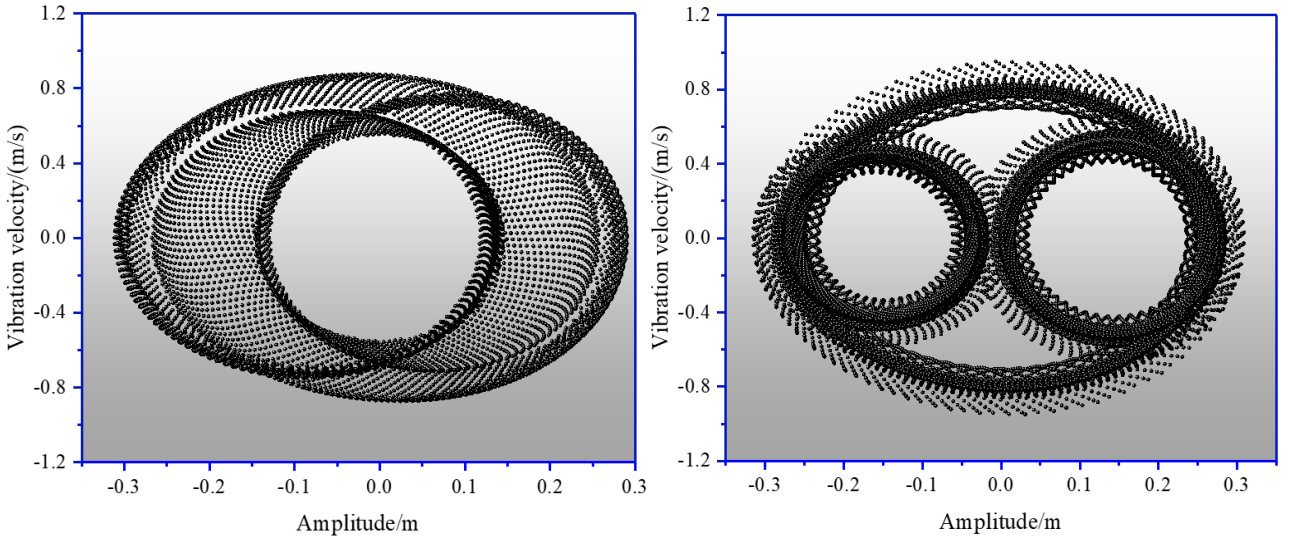

(b) Excitation amplitude p=1(3 000-3 800 s)　　(c) Excitation amplitude p=2(0-2 000 s)

Fig. 8　The time history displacement curve and phase diagram

5.4　Numerical Solution of 1/2-order Sub-harmonic Resonance

When the frequency of the periodic excitation is equal to twice the natural frequency of the system, the resonance of the system is called the 1/2-order sub-harmonic resonance.

When the excitation amplitude p=0.4, the limit cycle of the forced-self-excited system excited by the 1/2-order sub-harmonic is a closed elliptic cycle. Compared with the Fig. 5(a), in Fig. 9(a), the galloping time(t) of the history displacement curves is 1 000 s, and the galloping velocity of the system changes faster with the galloping amplitude when the amplitude is less than zero. As the excitation amplitude p=28, it can be seen from Fig. 9(b) that the galloping time(t) of the history displacement curves is 25 s; the galloping amplitude and galloping velocity also increase to -2.172 m and -10.228 m/s, and the phase diagram is the heart shape with one intersection point. As the excitation amplitude increases to p=38, it can be seen from Fig. 9(c) that the galloping time(t) of the history displacement curves is 35 s; the galloping amplitude and galloping velocity decrease to -1.963

m, -10.337 m/s, and the phase diagram changes from the one periodic motion to period-two periodic motion gradually. When the excitation amplitude increases to p=48, it can be seen from Fig. 9(d) that the galloping amplitude and galloping velocity decrease to -1.510 m and 8.936 m/s, and the phase diagram changes from the period-two periodic motion to the closed elliptic ring with period-one periodic motion gradually.

In Fig. 9, from Fig. 9(a) to Fig. 9(b), and then to Fig. 9(c) and Fig. 9(d), with the increase in excitation amplitude, it can be seen that the galloping amplitude of the forced-self-excited system with 1/2-order sub-harmonic resonance increases first and then decreases; the phase diagram first changes from a closed elliptic ring to a concave heart shape, then changes to period-two periodic motion, and finally changes to period-one periodic motion.

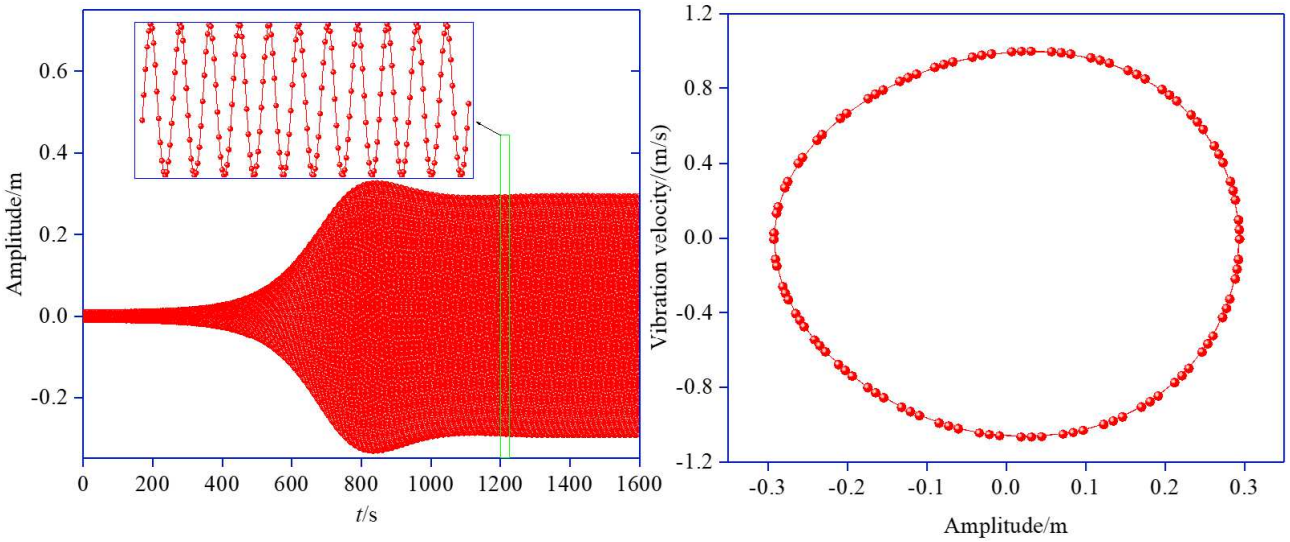

(a) Excitation amplitude p=0.4

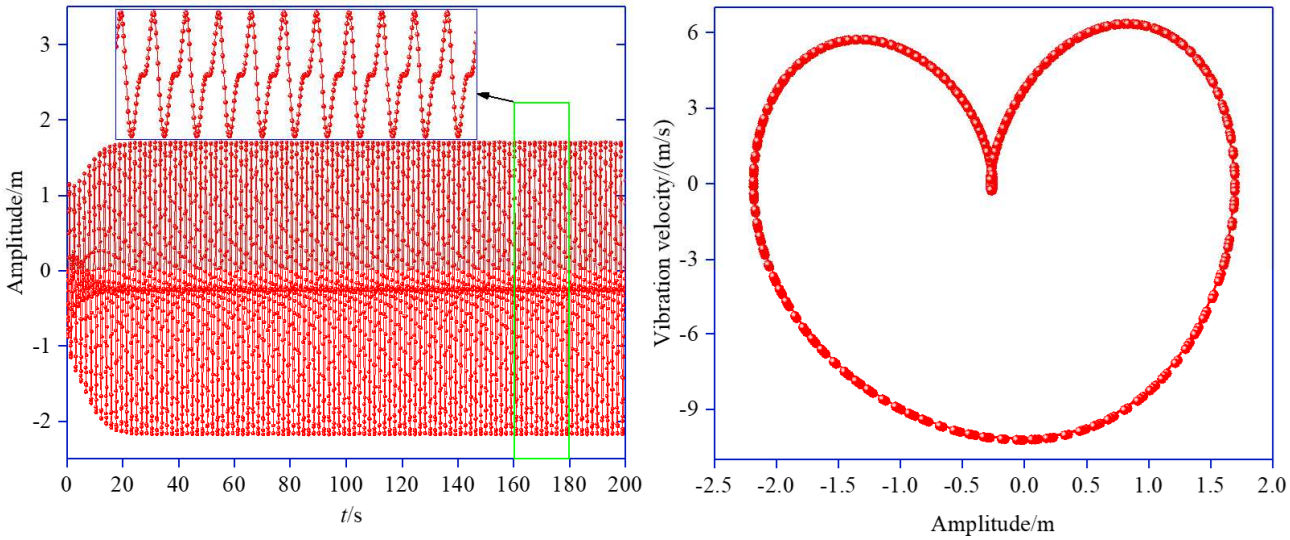

(b) Excitation amplitude p=28

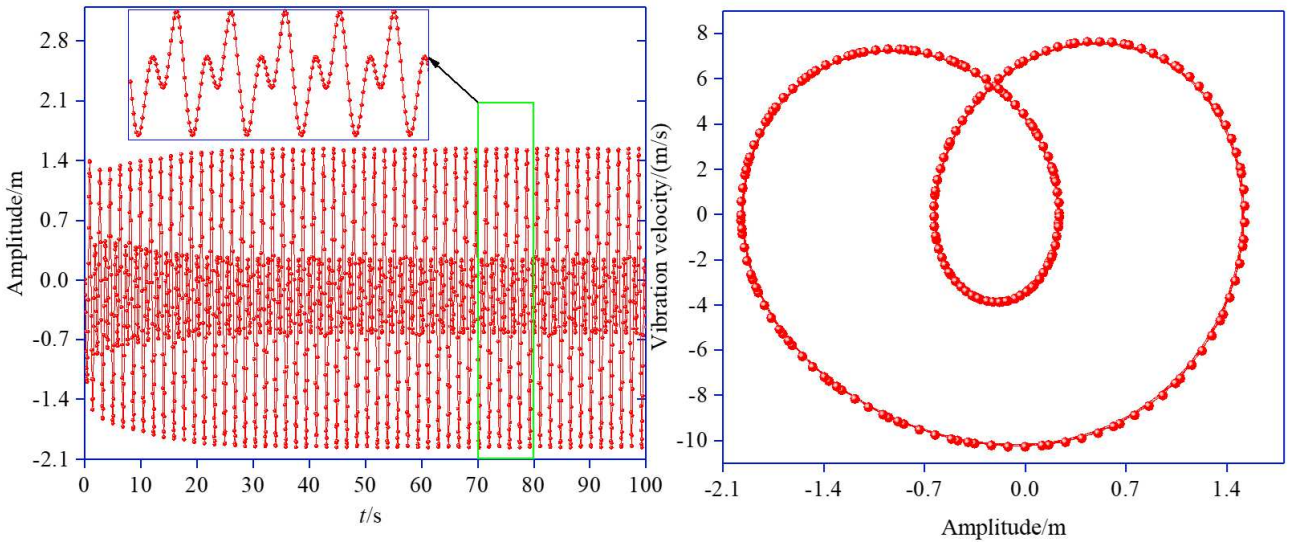

(c) Excitation amplitude p=38

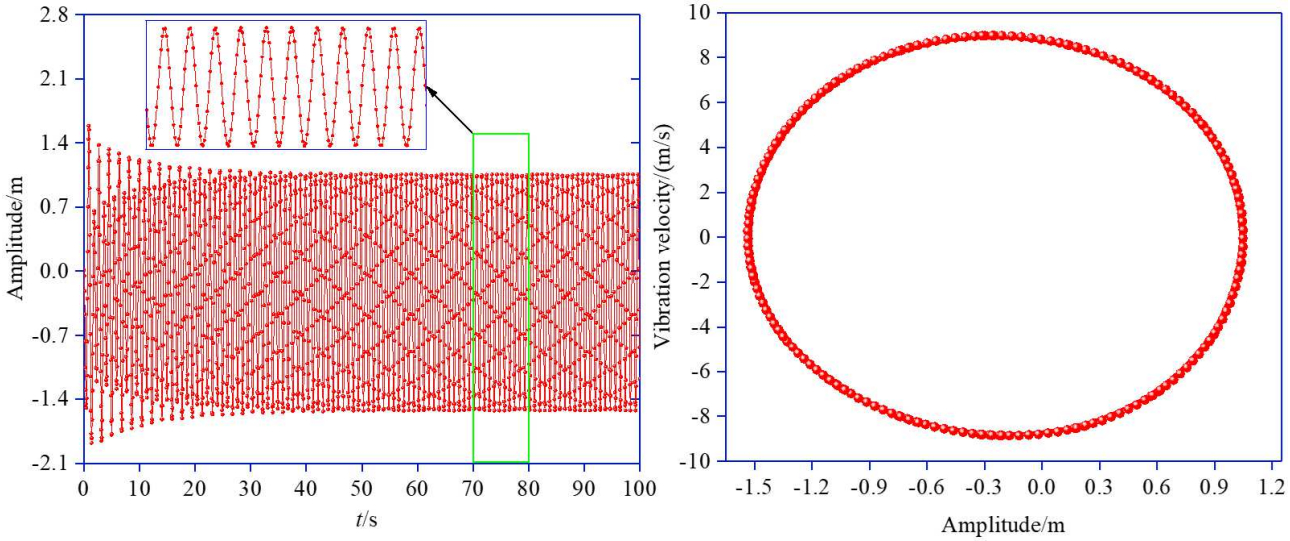

(d) Excitation amplitude p=48

Fig. 9 The time history displacement curve and phase diagram

5.5 Numerical Solution of 1/3-order Sub-harmonic Resonance

When the frequency of the external excitation is equal to three-times natural frequency of the system, the resonance of the system is called the 1/3-order sub-harmonic resonance.

As the excitation amplitude p=2, the limit cycle of the forced-self-excited system excited by the 1/3-order sub-harmonic is also a closed elliptic cycle. Compared with Fig. 5(a), the beat vibration phenomenon of forced vibration becomes more obvious in Fig. 10(a).

When the excitation amplitude p=4, it can be seen from Fig. 10(b) that the galloping time(t) of the history displacement curves is 2 000 s; the galloping amplitude and galloping velocity are -0.187 m and 0.774 m/s; the upper and lower sides of the phase diagram curve are concave. In Fig. 10(c), as the excitation amplitude increases to p=5, it is easy to see that the phase diagram increases from the period-one periodic motion to period-three periodic motion, and the galloping amplitude and galloping velocity decrease to -0.078 m and -0.613 m/s. In Fig. 10(d), when the excitation amplitude

increases to p=16, it can be seen that the galloping amplitude and galloping velocity increase to -0.168 m and 1.729 m/s, and the phase diagram changes from the shape of period-three periodic motion to the closed elliptic ring with period-one periodic motion gradually.

When the excitation amplitude increases to p=50, it can be seen from Fig. 10(e) that the galloping amplitude and galloping velocity increase to -0.564 m and 5.426 m/s, the phase diagram still maintains the closed elliptic ring shape with period-one periodic motion, and the galloping time(t) of the history displacement curves is 8 s.

In Fig. 10, with the increase in excitation amplitude, from Fig. 10(a) to Fig. 10(b), and then to Fig. 10(c), it can be seen that the galloping amplitude of the system with 1/3-order sub-harmonic resonance first decreases and then increases. And the phase diagram changes from a closed elliptic ring to a concave shape with two intersection points, then to period-three periodic motion, and to a closed elliptic ring with period-one periodic motion finally.

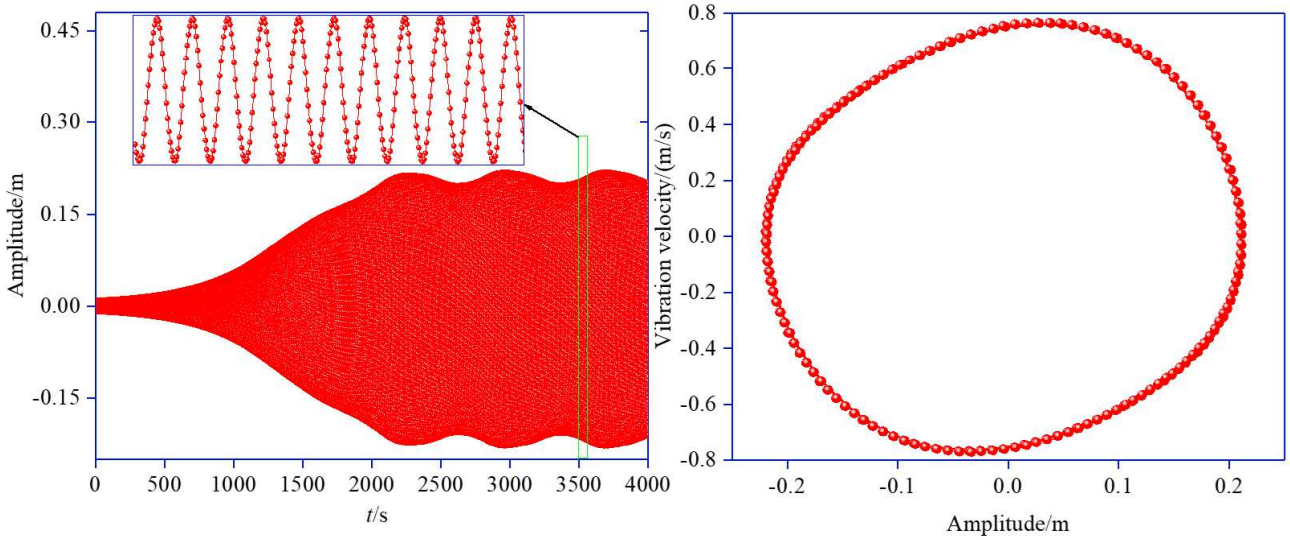

(a) Excitation amplitude p=2

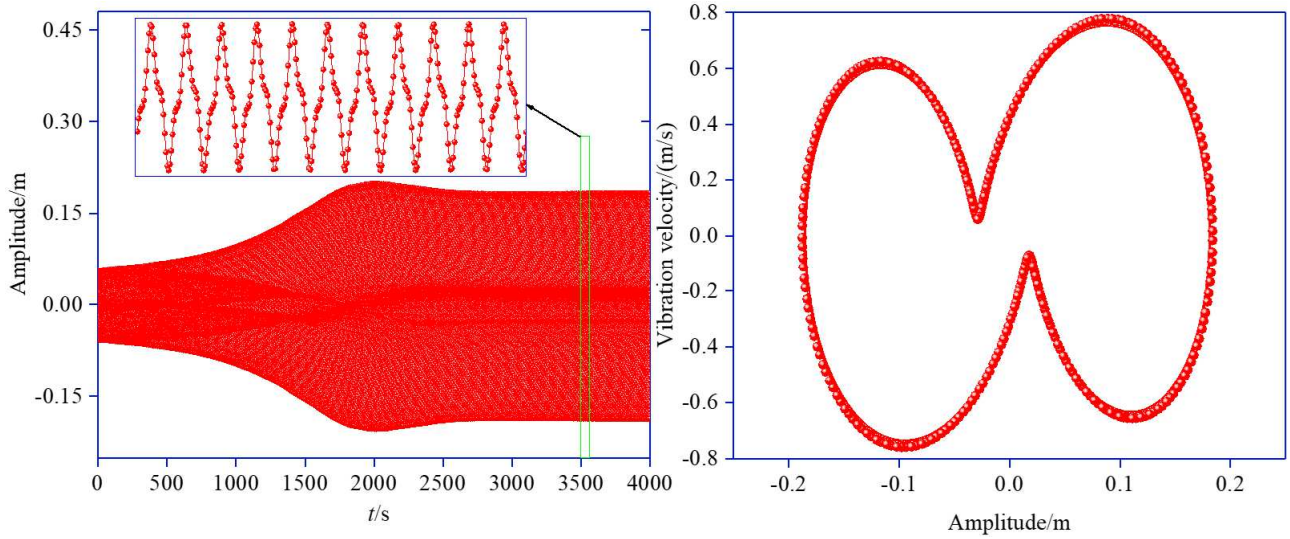

(b) Excitation amplitude p=4

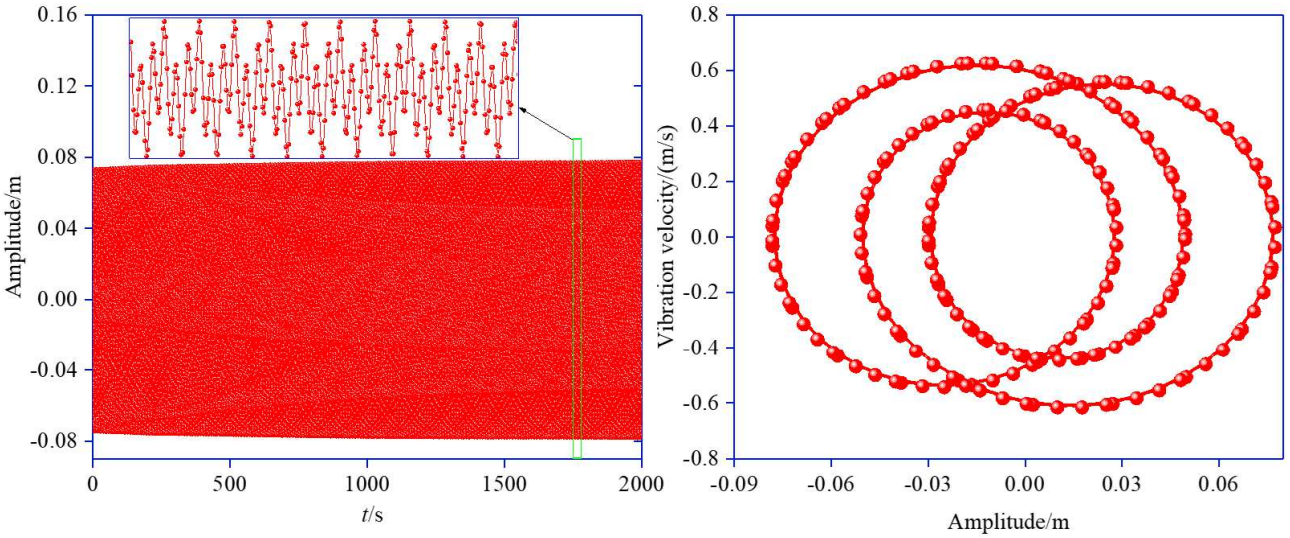

(c) Excitation amplitude p=5

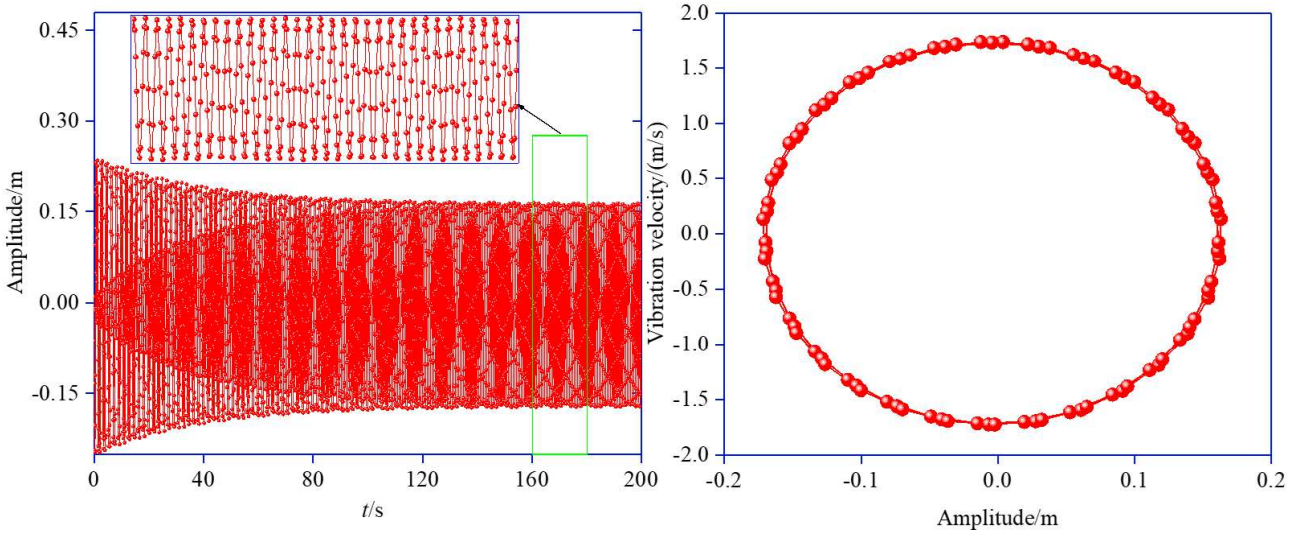

(d) Excitation amplitude p=16

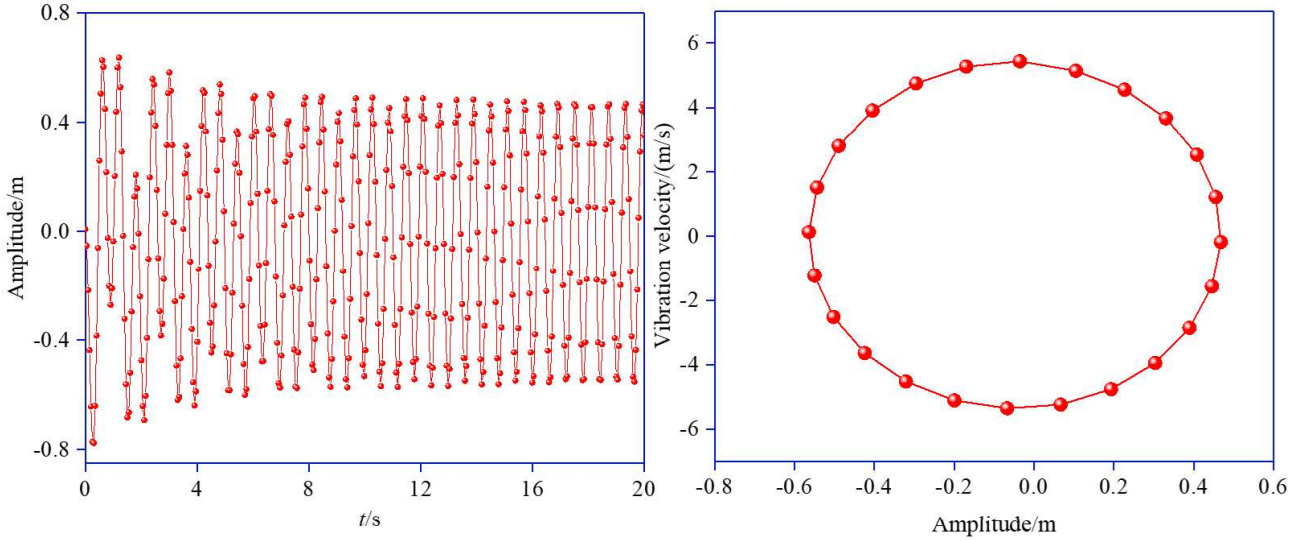

(e) Excitation amplitude p=50

Fig. 10 Time history displacement curve and phase diagram

Fig. 5, Fig. 6, Fig. 7, Fig. 9, and Fig. 10 correspond to the principal resonance, 2-order super-harmonic resonance, 3-order super-harmonic resonance, 1/2-order sub-harmonic resonance and 1/3-

order sub-harmonic resonance of the forced-self-excited system respectively. From the analysis of the galloping time, galloping amplitude, and galloping velocity of the time history displacement diagram in section 5.1 to section 5.5, it can be seen that: for the principal resonance and super-harmonic resonance, with the increase in the excitation amplitude, the galloping amplitude and galloping velocity of the forced-self-excited system continue to increase, and the galloping time continues to decrease; for the sub-harmonic resonance, with the increase in excitation amplitude, the galloping amplitude and galloping velocity of forced-self-excited system first decrease and then increase. Compared with the harmonic resonance and the principal resonance, the principal resonance response increases the most, and the increase of sub-harmonic resonance response is the smallest. Under the condition of same physical parameters and same external excitation, the principal resonance can cause galloping of iced transmission line in the shortest time, and the galloping amplitude and galloping velocity are also the largest; the super-harmonic resonance takes the second place; however, the sub-harmonic resonance may reduce the response of the system. Therefore, for the transmission line structure, the harm of principal resonance is greater than that of super harmonic resonance, and the harm of super harmonic resonance is greater than that of sub harmonic resonance.

Fig. 11 shows the time history displacement image and phase diagram of the 1/3-order sub-harmonic resonance of the system under different excitation amplitudes. In Fig. 11(a), Fig. 11(b), and Fig. 11(c), the left figures show the time history displacement diagram of the system when the excitation amplitude p=0.5, p=3, and p=5.2, respectively; and the right figure shows the phase diagram of the rectangular frame part of the dotted line in the left figure.

In Fig. 11(a) and Fig. 11(b), as the excitation amplitude increases from p=0.5 to p=3, the forced-self-excited system is the superposition form of forced vibration and self-excited vibration, in which the phenomenon of beat vibration in time history displacement becomes very obvious gradually. In Fig. 11(c), while excitation amplitude increases to p=5.2, the beat phenomenon of time history displacement disappears; the self-excited vibration characteristic of time history displacement disappears, and the quenching phenomenon also appears.

In Fig. 11, from Fig. 11(a) to Fig. 11(b), and then to Fig. 11(c), the external excitation effect in the system is enhanced, and the phase diagram change from the form of beat vibration to quasi-periodic vibration with period-three periodic motion gradually.

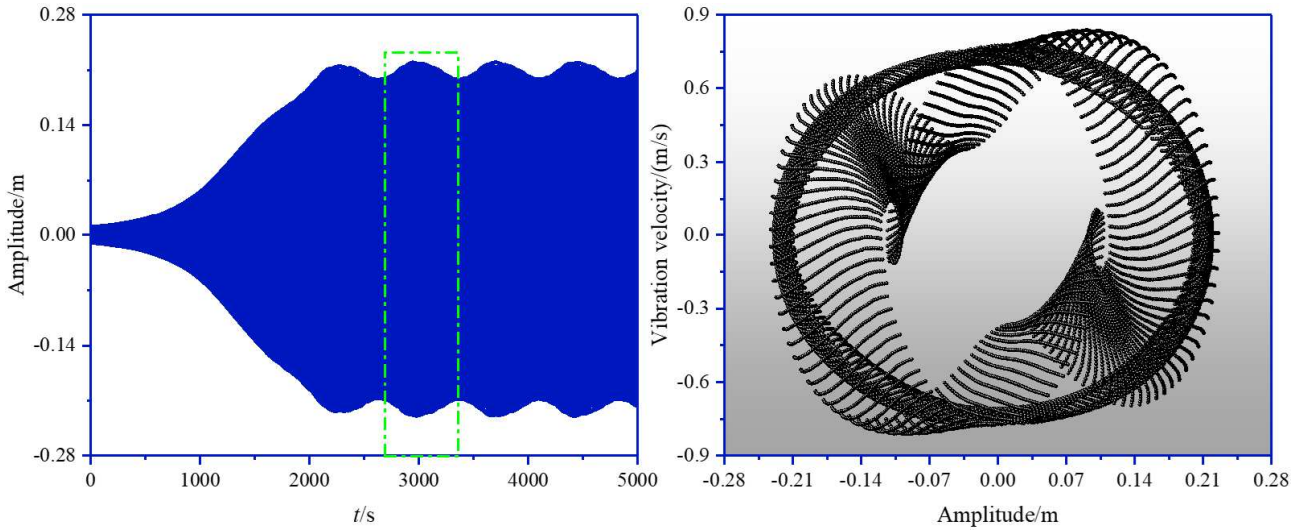

(a) Excitation amplitude p=0.5(2700-3300)

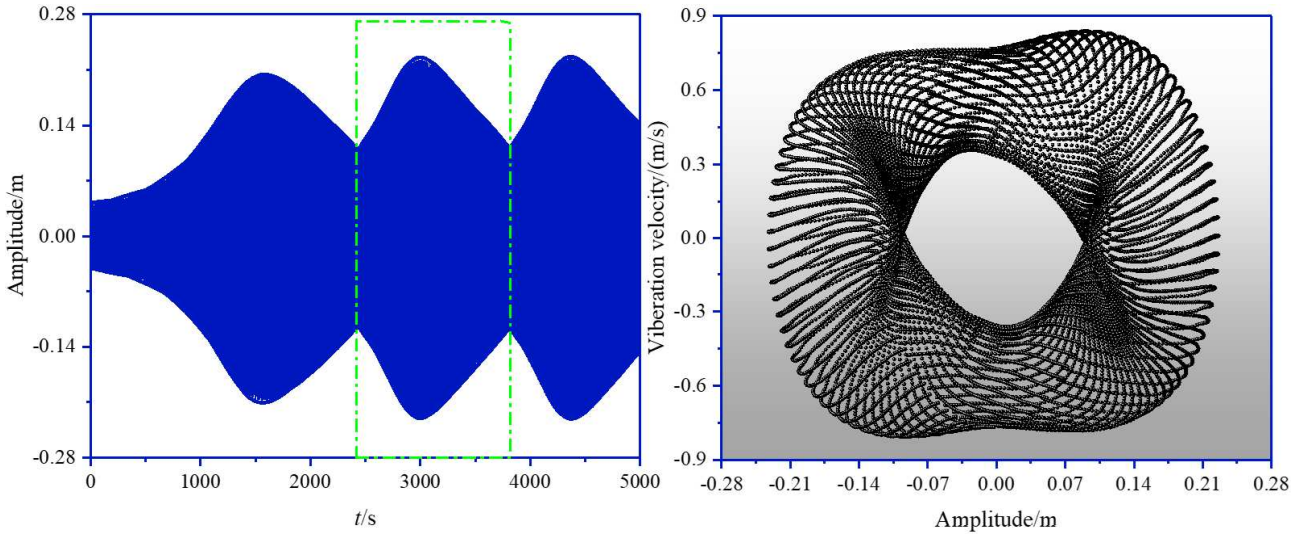

(b) Excitation amplitude p=3(2400-3800)

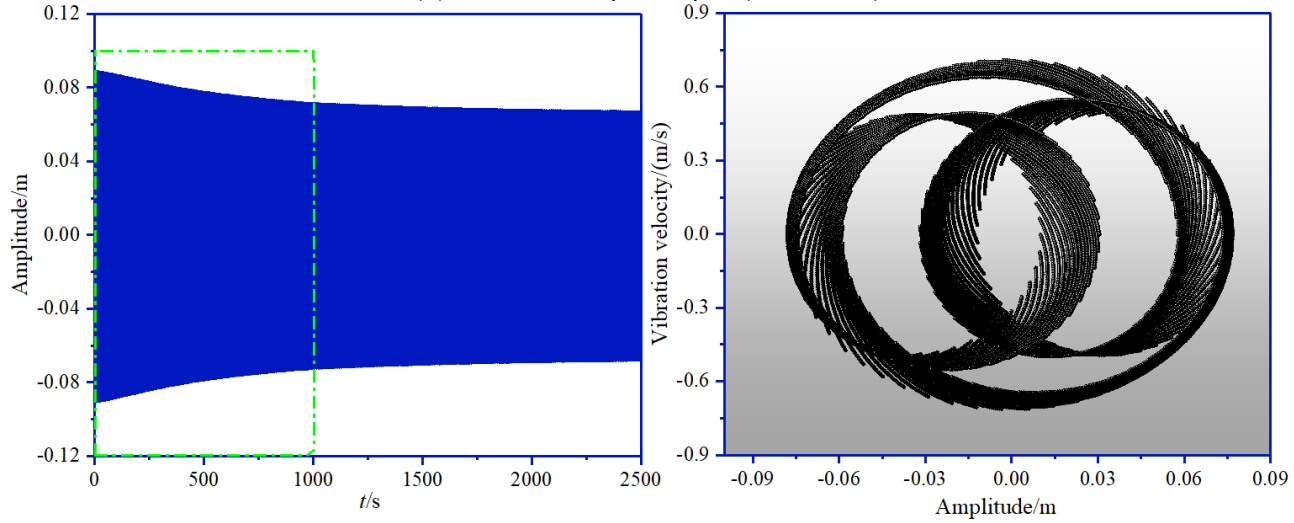

(c) Excitation amplitude p=5.2(0-1000)

Fig. 11 The time history displacement curve and phase diagram

6 Conclusion

By establishing the physical model of iced transmission line under the condition of dynamic

wind, a new forced self-excited system is obtained. The multiple scale method is used to solve the forced-self-excited system, and the periodic approximate analytical solution (non-resonance) and amplitude-frequency response relation (principal resonance) are obtained. By comparing the approximate analytical solution with the numerical solution, the applicability of the approximate analytical solution is obtained. Then, the time history displacement curves and phase diagrams of different excitation frequencies and different excitation amplitudes are obtained by numerical method. The results show that the forced-self-excited system has different harmonic resonance forms due to different excitation frequencies:

(1) For the forced-self-excited system, when the excitation amplitude is equal to 0, the vibration form of the system is pure self-excited vibration; when the excitation amplitude $p>0$, the vibration form of the system is expressed as the superposition form of self-excited vibration and forced vibration; when the excitation amplitude (p) is greater than the critical value, the self-excited vibration disappears, resulting in quenching phenomenon, the vibration form of the system is forced vibration regulated by Rayleigh damping.

(2) With the increase of external wind velocity and excitation amplitude, the forced-self-excited system changes from weak nonlinear system to strong nonlinear system, so the accuracy of approximate analytical solution of the multiple scales method is reduced.

(3) For super-harmonic resonance, the system of transmission line excited by 2-order super-harmonic excitation produces the vibration form with period-two period motion; the system of transmission line excited by 3-order super-harmonic excitation produces the vibration form with period-three period motion; and with the increase of excitation amplitude, the galloping time of the system can be reduced to 20 s, and the vibration amplitude also increases sharply.

(4) With the increase in excitation amplitude, the phase diagram of the iced transmission line system under 1/2-order sub-harmonic excitation produces an intersection point, which changes from period-one period motion to period-two periodic motion; and the phase diagram of the iced transmission line system under 1/3-order sub-harmonic excitation produces two intersection points, which changes from one periodic motion to period-three periodic motion. When the amplitude is greater than the critical value, the iced transmission line system under sub-harmonic excitation will change from the vibration form of period-two, and period-three period motion to the vibration form of period-one period motion.

(5) With the increase in excitation amplitude, the 3-order super-harmonic resonance and 1/3-order sub-harmonic resonance will undergo meaningful transition from periodic vibration to quasi periodic vibration and then to periodic vibration. For the forced-self-excited system of the iced transmission line, the harm of the principal resonance is greater than that of the super-harmonic resonance, and the harm of the super-harmonic resonance is greater than that of the sub-harmonic resonance. Therefore,

in practical engineering application, the physical parameters of transmission line should be adjusted to make the natural frequency far away from the frequency region of principal resonance and super-harmonic resonance.

Conflicts of Interest

The authors declare that there are no conflicts of interest regarding the publication of this paper.

Data availability statement

The authors declare that the data are available regarding the publication of this paper.

Acknowledgments

This work was financially supported by the National Natural Science Foundation of China (51507106 and 51308570), Cutting Edge Project of Chongqing Science and Technology Commission (cstc2017jcyjAX0246), Graduate Research and Innovation Project of Chongqing (cys19240), China Postdoctoral Science Foundation (2720M672238), Chengdu International Science and Technology Cooperation Support Funding (2720-GH02-00059-HZ) and Technology Research Project of Chongqing Education Commission (KJ201600712182).

ORCID

Xiaohui Liu: https://orcid.org/0000-0002-2299-9279

Shuguang Yang: https://orcid.org/0000-0002-4554-4795

Guangyun Min: https://orcid.org/0000-0002-4043-7480

Ceshi Sun: https://orcid.org/0000-0002-9970-4539

Haobo Liang: https://orcid.org/0000-0002-8866-9504

Ming Zou: https://orcid.org/0000-0002-9091-1304

Chuan Wu: https://orcid.org/0000-0002-4920-0412

Mengqi Cai: https://orcid.org/0000-0002-1941-0179

References：

1 Liu, X.H., Liu, L., Cai, M.Q., Yan, B.: Free vibration of transmission lines with multiple insulator strings using refined models. Appl. Math. Model. **67**, 252-282(2019)

2 Yan, B., Liu, X.H., Lv, X., Zhou, L.S.: Investigation into galloping characteristics of iced quad bundle conductors. J. Vib. Control. **22**, 968–987(2016)

3 Lou, W.J., Wang, J.W., Chen, Y., Lv, Z.B., Lu, M.: Effect of motion path of downburst on wind-induced conductor swing in transmission line. Wind Struct. **23**, 41–59(2016)

4 Krarup, N. H., Zhang, Z., Kirkegaard, P. H.: Active modal control of rain-wind induced vibration of stay cables. Procedia Eng. **199**, 3158-3163(2017)

5 McTavish, S., Raeesi, A., D'Auteuil, A., Yamauchi, k., Sato, H.: An investigation of the mechanisms causing large-amplitude wind-induced vibrations in stay cables using unsteady surface pressure measurements. J. Wind Eng. Ind. Aerod. **183**, 19-34(2018)

6 Arafat, H. N., Nayfeh, A. H.: Non-linear responses of suspended cables to primary resonance excitations. J. Sound Vib. **266**, 325-354(2003)

7 Kamel, M. M., Hamed, Y. S.: Nonlinear analysis of an elastic cable under harmonic excitation. Acta Mech. Sinica. **214**, 315-325(2010)

8 Kang, H.J., Zhu, H.P., Zhao, Y.Y., Yi, Z.P.: In-plane non-linear dynamics of the stay cables. Nonlinear Dyn. **73**, 1385-1398(2013)

9 Zhao, Y.B., Sun, C.S., Wang, Z.Q., Wang, L.H.: Analytical solutions for resonant response of suspended cables subjected to external excitation. Nonlinear Dyn. **78**, 1017-1032(2014)

10 Nayfeh, A.H., Arafat, A.H., Chin, C.M., Lacarbonara, W.: Multimode interactions in suspended cables. J. Vib. Control. **8**, 337–387 (2002)

11 Rega, G., Benedettini, F.: Planar non-linear oscillations of elastic cables under subharmonic resonance conditions. J. Sound Vib. **132**, 367–381 (1989)

12 Rega, G., Benedettini, F.: Planar nonlinear oscillations of elastic cables under super harmonic resonance conditions. J. Sound Vib. **132**, 353–356 (1989)

13 Chen, H.K., Zuo, D.H., Zhang, Z.H., Qing, X.: Bifurcations and chaotic dynamics in suspended cables under simultaneous parametric and external excitations. Nonlinear Dyn. **62**, 623-646(2010)

14 Zhang, W., Tang, Y.: Global dynamics of the cable under combined parametrical and excitations. Int. J. Nonlin. Mech. **37**, 505–526 (2002)

15 Perkins, N.C.: Modal interaction in the nonlinear response of elastic cables under parametric/external excitation. Int. J. Nonlin. Mech. **27,** 233–254(1992)

16 Sun, C.S., Zhou, X.K., Zhou, S.X.: Nonlinear responses of suspended cable under phase-differed multiple support excitations. Nonlinear Dyn. **65**, 1-20(2021)

17 Berlioz, A., Lamarque, C.-H.: A non-linear model for the dynamics of an inclined cable. J. Sound Vib. **279**, 619-639(2005)

18 Wu, Q., Takahashi, K., Nakamura, S.: Formulae for frequencies and modes of in-plane vibrations of small-sag inclined cables. J. Sound Vib. **279**, 1155–1169(2005)

19 Daniele, Z., Luongo, A.: Bifurcation and stability of a two-tower system under wind-induced parametric, external and self-excitation. J. Sound Vib. **331**, 365-383(2012)

20 Angelo, L., Daniele, Z.: Parametric, external and self-excitation of a tower under turbulent wind

flow. J. Sound Vib. **330**, 3057–3069(2011)

21 Liu, X.H., Yang, S.G., Wu, C., Zou, M., Min, G.Y., Sun, C.S., Jiang, Y.T.: Planar nonlinear galloping of iced transmission lines under forced self-excitation conditions. Discrete Dyn. Nat. Soc. **2021**, 1-20(2021)

22 Irvine, H.M., Caughey, T.K.: The linear theory of free vibration of suspended cable. P. Roy. Soc. Lond. A. Mat. **341**, 299-315(1974)

23 Liu, X.H., Zou, M., Wu, C., Cai, M.Q., Min, G.Y., Yang, S.G.: Galloping Stability and Wind Tunnel Test of Iced Quad Bundled Conductors Considering Wake Effect. Discrete Dyn. Nat. Soc. **2020**, 1-18(2020)

24 Den Hartog, J.: Transmission lines vibration due to sleet. Transactions of the American Institute of Electrical Engineers. **51**, 1074-1076(1933)

25 Min, G.Y., Liu, X.H., Wu, C., Yang, S.G., Cai, M.Q.: Influences of Two Calculation Methods About Dynamic Tension on Vibration Characteristics of Cable-Bridge Coupling Model. Discrete Dyn. Nat. Soc, **2021**, 1-11(2021)

26 Liu, X.H., Yang, S.G., Min, G.Y., Wu, C., Cai, M.Q.: Investigation on the accuracy of approximate solutions obtained by perturbation method for galloping equation of iced transmission lines. Math. Probl. Eng. **2021**, 1-18(2021)

27 Nielsen, S.R.K., Kirkegaard, P.H.: Super and combinatorial harmonic response of flexible elastic cables with small sag. J. Sound Vib. **251**, 79-102(2002)

28 Zhang, Q., PoppleWell, N., Shah, A. H.: Galloping of bundle conductor. J. Sound vib. **234**, 115-134(2000)

29 Benedettini, F., Rega, G.: Non-linear dynamics of an elastic cable under planar excitation. Int. J. Non-linear Mech. **22**, 497-509(1987)

Figures

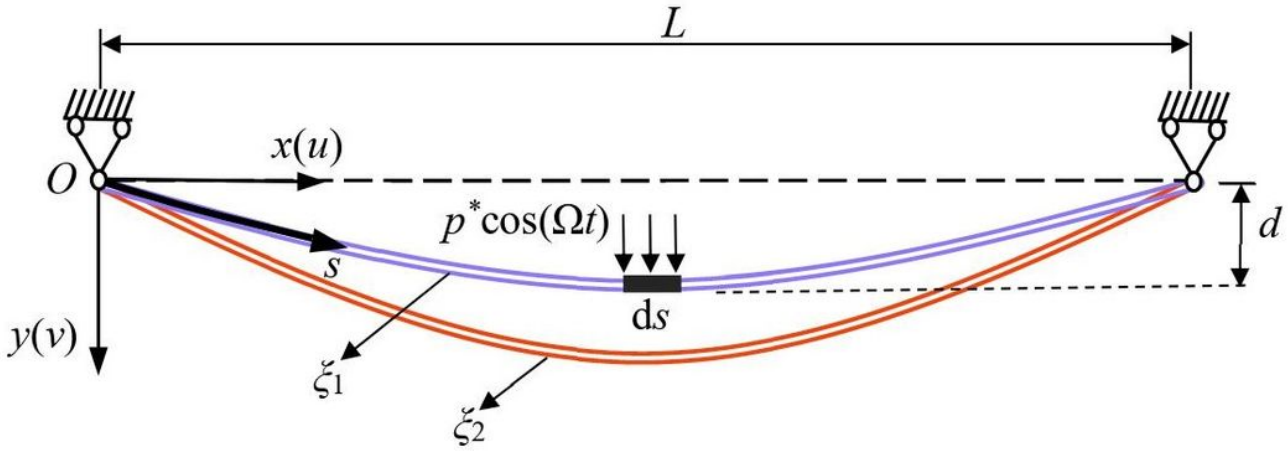

Figure 1

The model of singe-span equal-height transmission lines

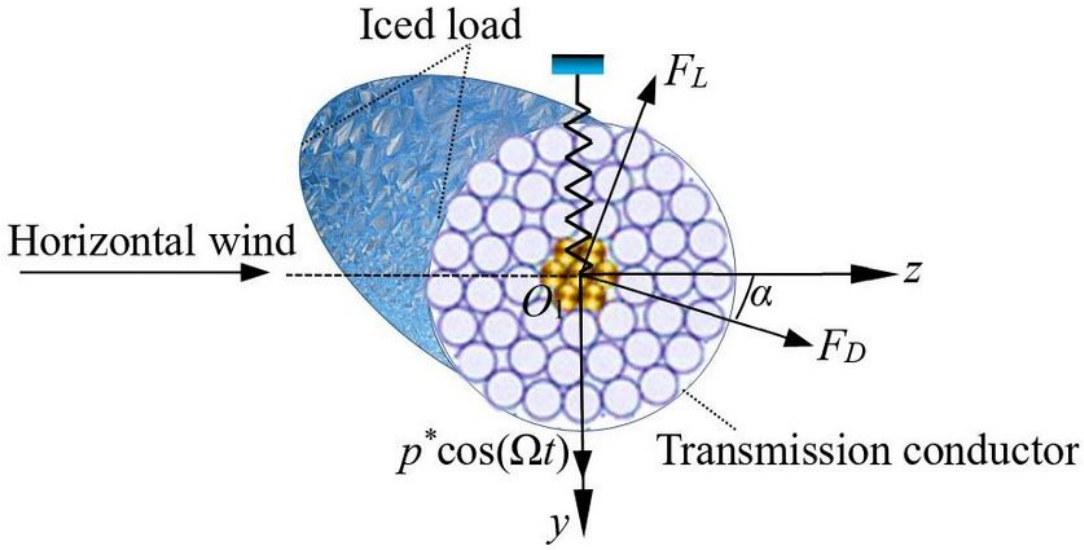

(a) The physical model

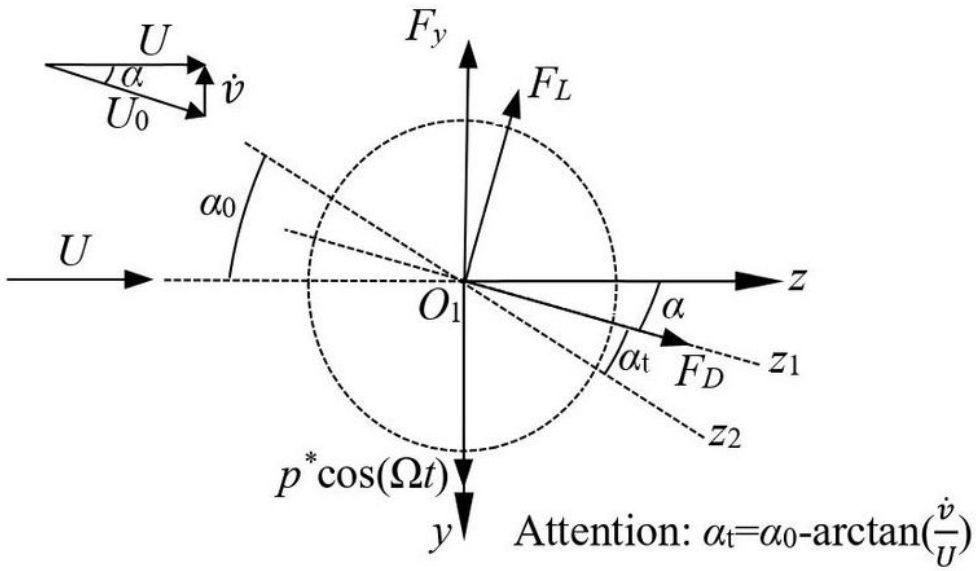

(b) The force analysis model

Figure 2

The model of cross-section of iced transmission lines

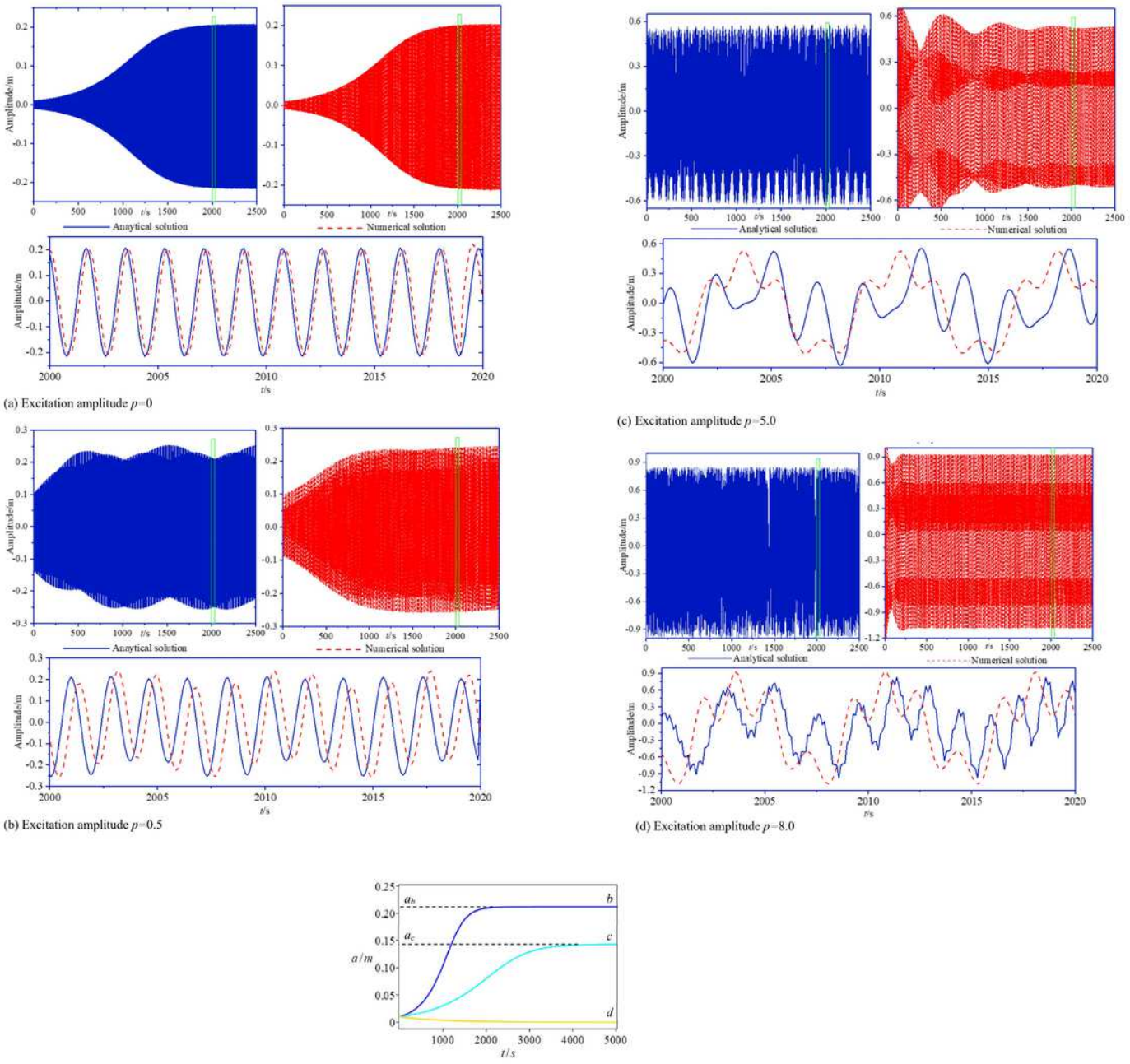

Figure 3

The time history displacement diagram of forced-self-excited system

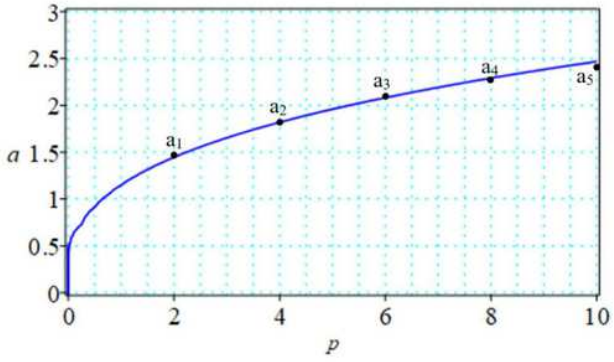

(a) U=4 m/s, H=30 000 N

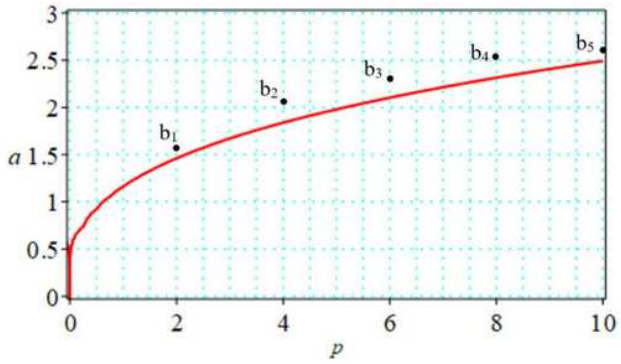

(b) U=8 m/s, H=30 000 N

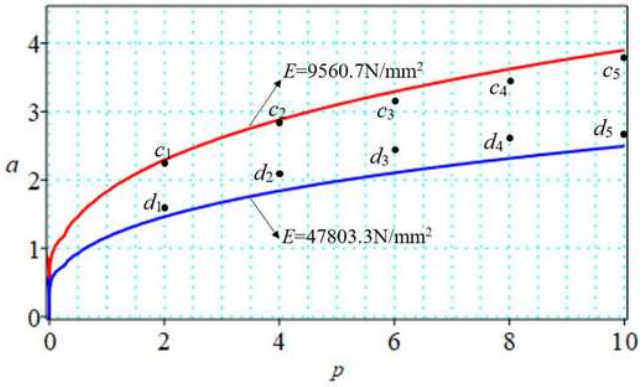

(c) U=8 m/s, H=30 000 N

Figure 4

The excitation amplitude(p)-response amplitude(a) curve

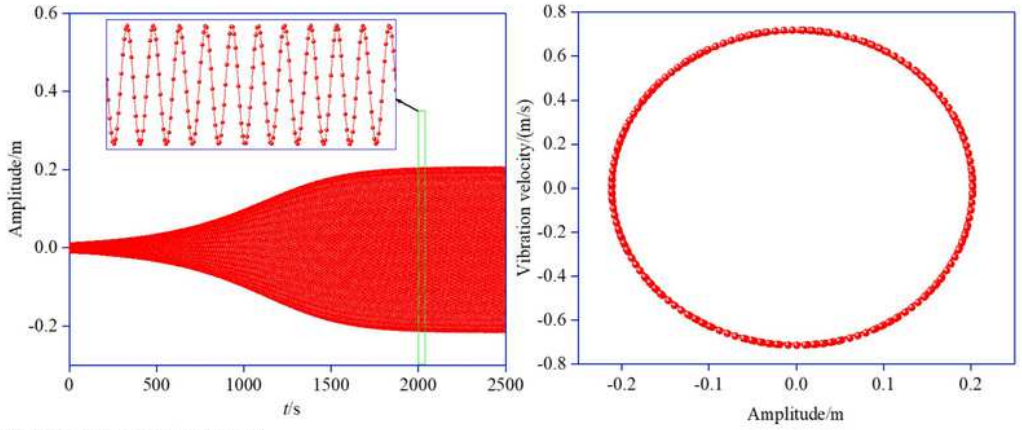

(a) Excitation amplitude p=0

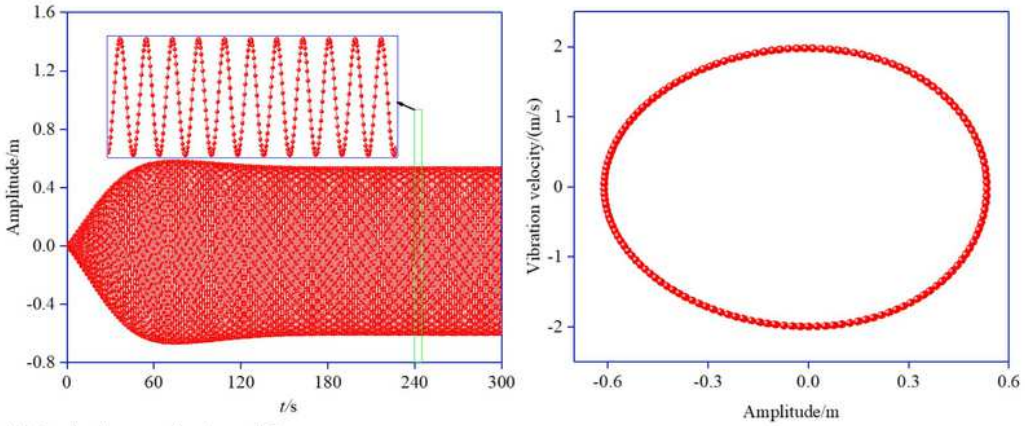

(b) Excitation amplitude p=0.1

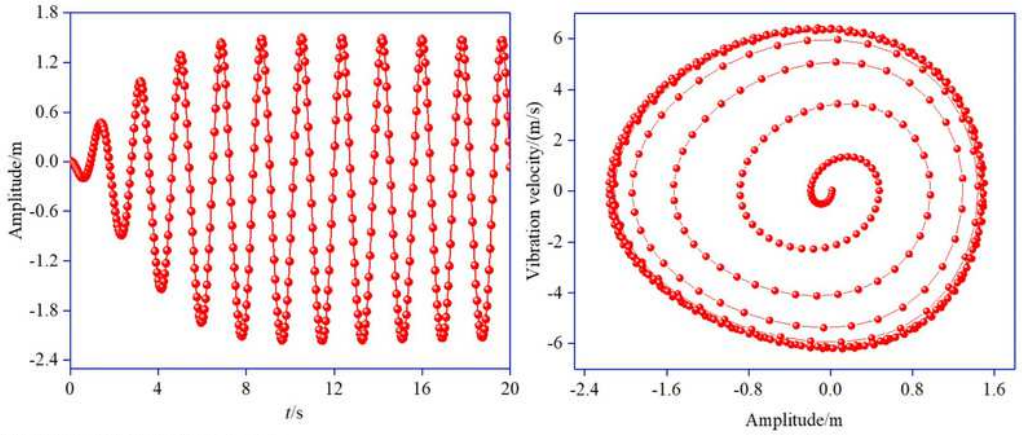

(c) Excitation amplitude p=2.5

Figure 5

The time history displacement curve and phase diagram

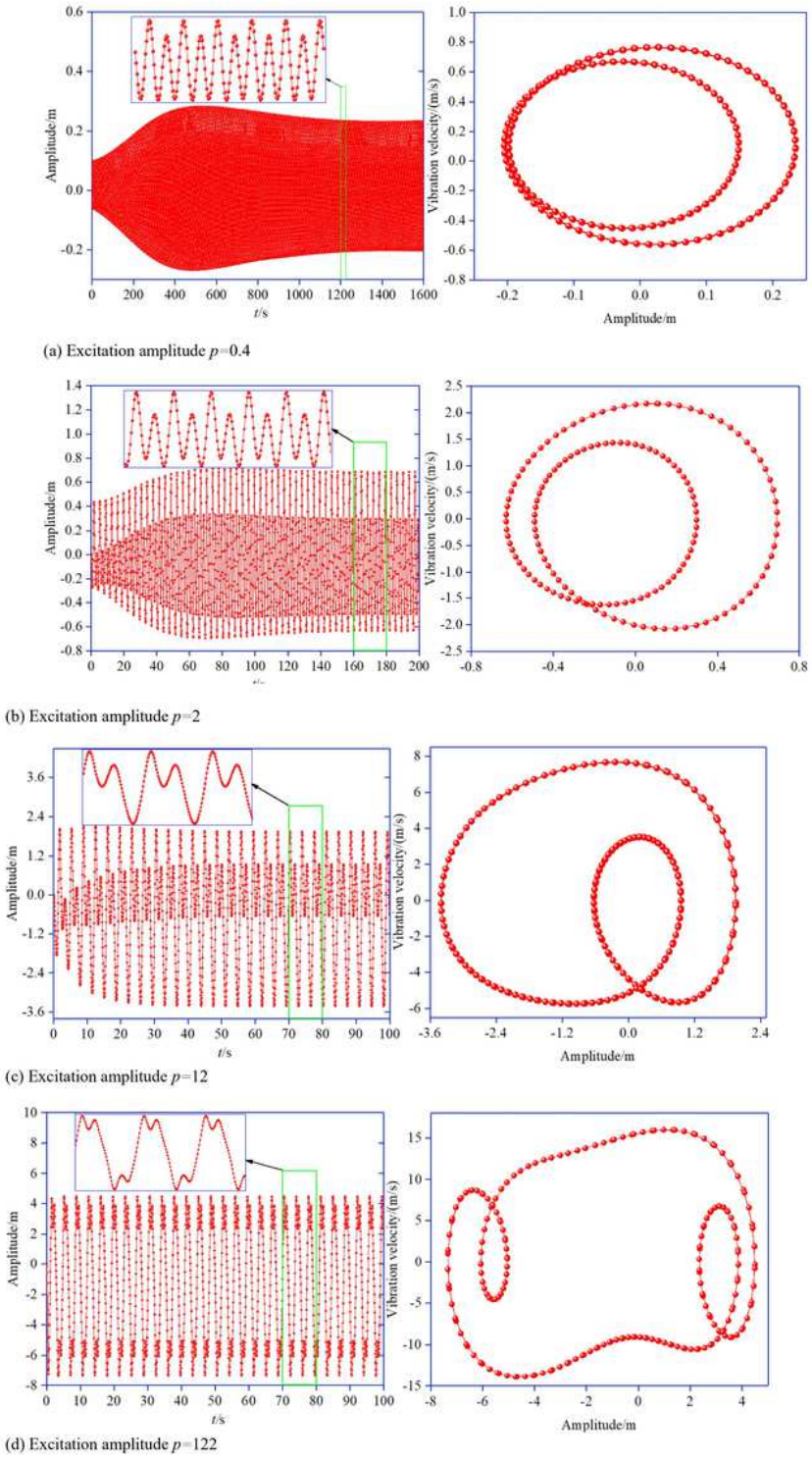

Figure 6

The time history displacement curve and phase diagram

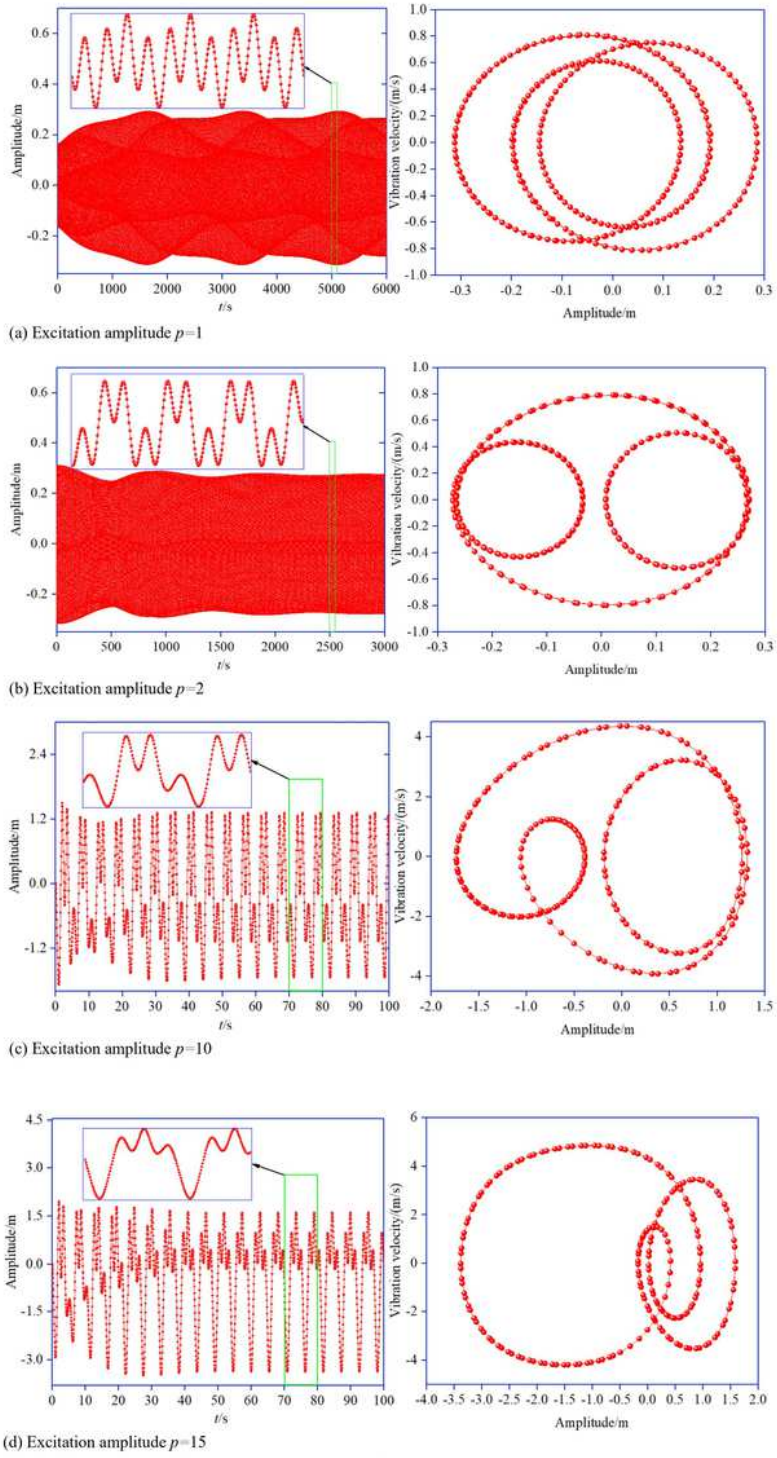

Figure 7

The time history displacement curve and phase diagram

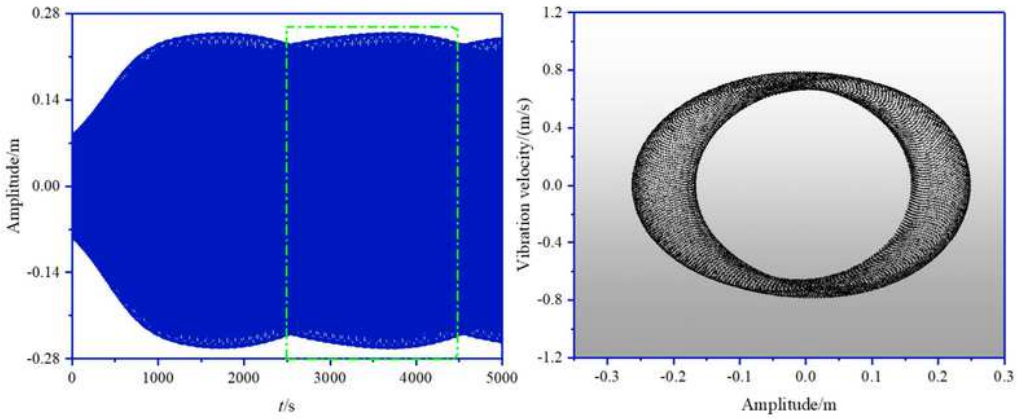

(a) Excitation amplitude p=0.5(2 500 -4 500 s)

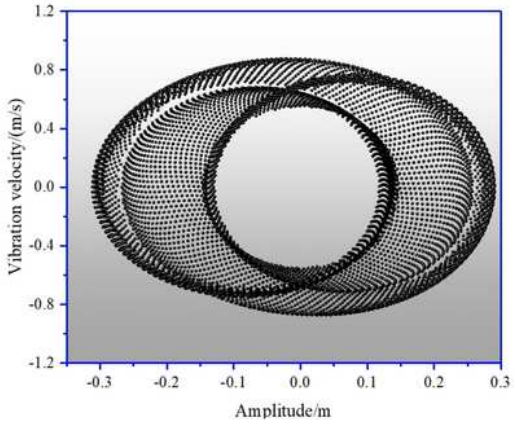

(b) Excitation amplitude p=1(3 000-3 800 s)

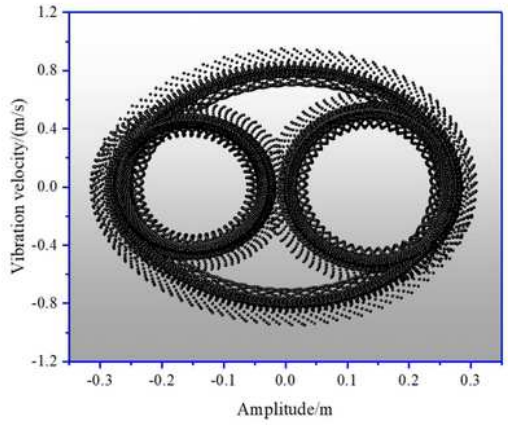

(c) Excitation amplitude p=2(0-2 000 s)

Figure 8

The time history displacement curve and phase diagram

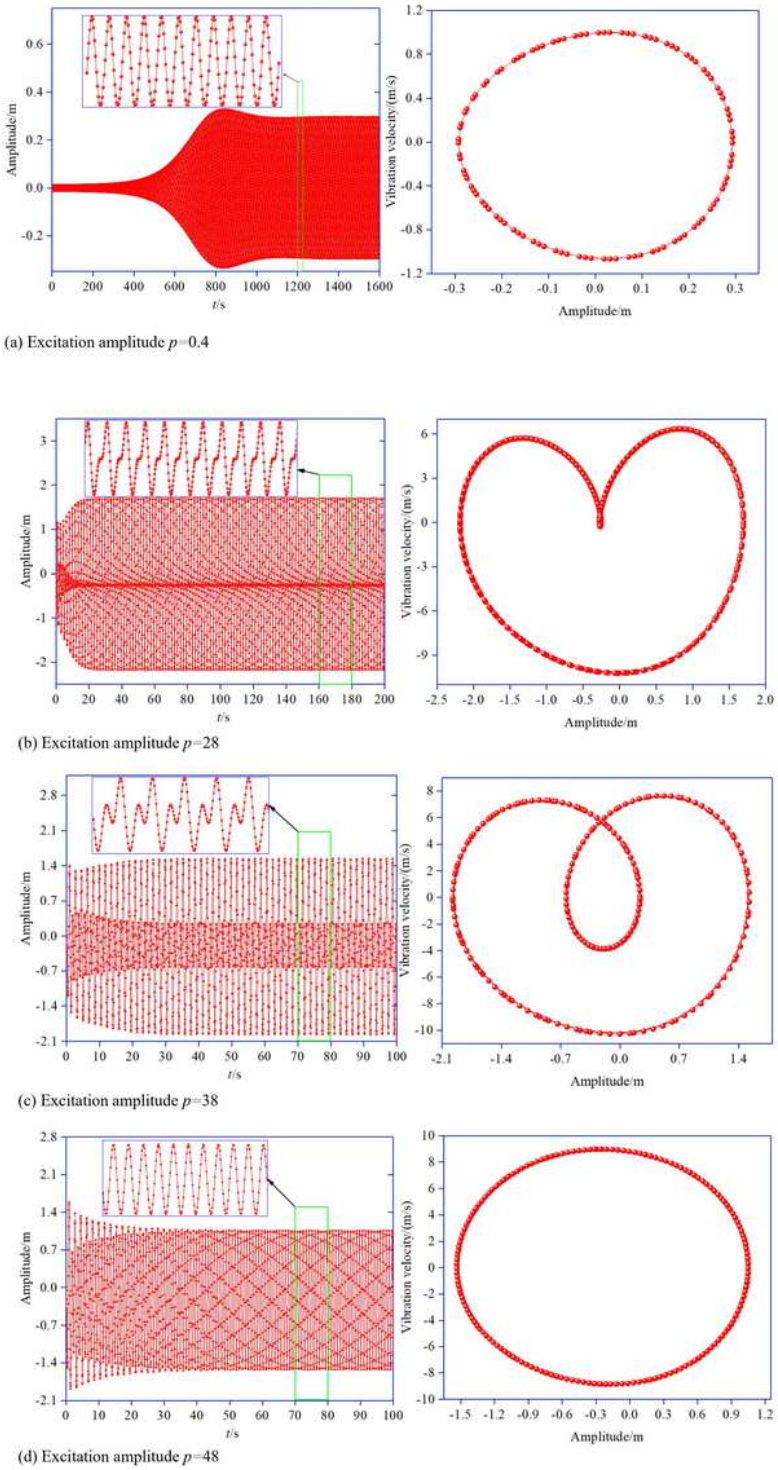

Figure 9

The time history displacement curve and phase diagram

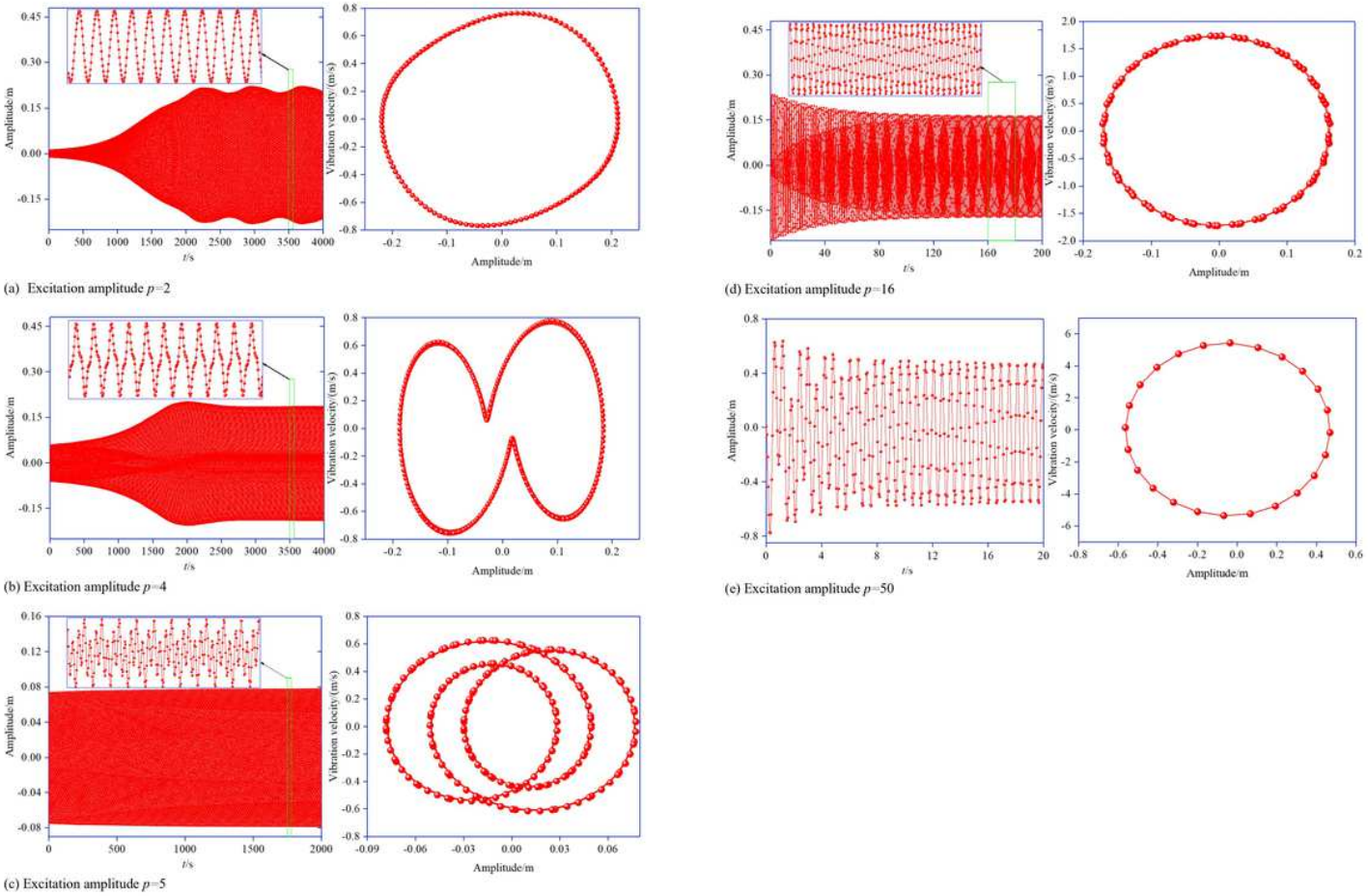

Figure 10

Time history displacement curve and phase diagram

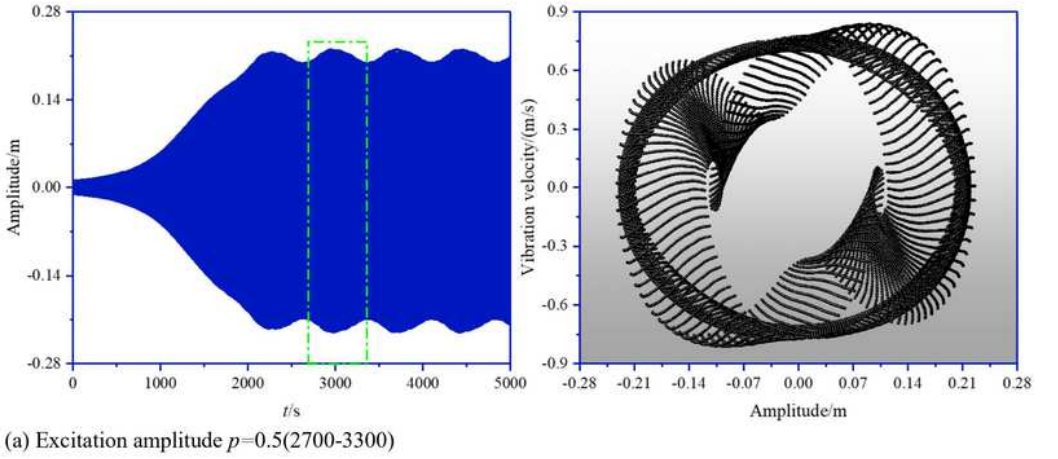

(a) Excitation amplitude p=0.5(2700-3300)

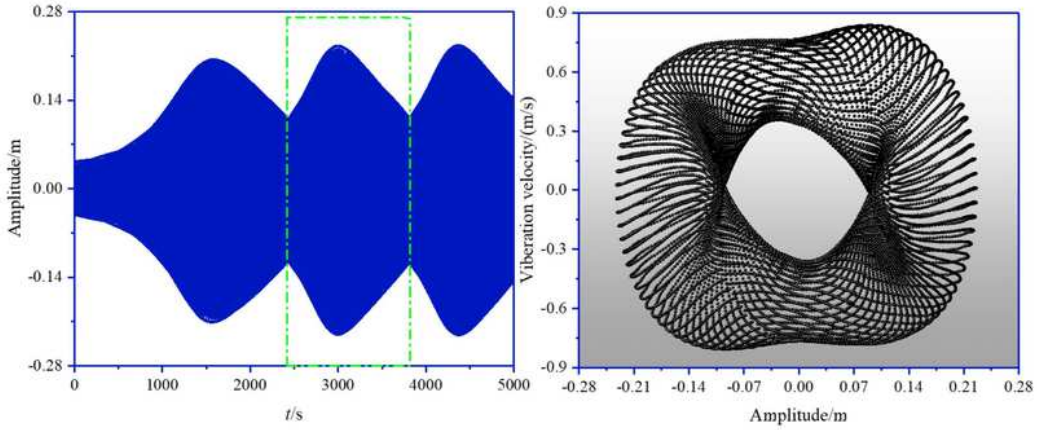

(b) Excitation amplitude p=3(2400-3800)

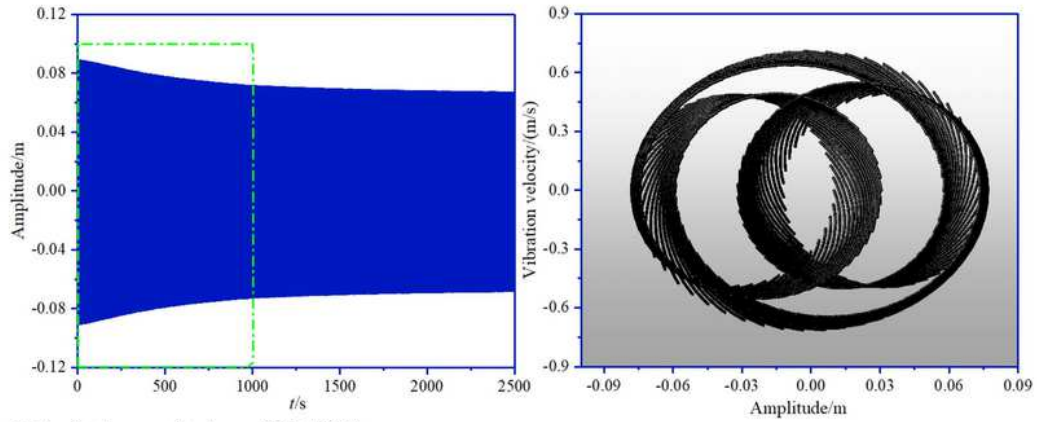

(c) Excitation amplitude p=5.2(0-1000)

Figure 11

The time history displacement curve and phase diagram

Supplementary Files

This is a list of supplementary files associated with this preprint. Click to download.

- Table.pdf